High-Resolution Environmagnetic Study of HOTRAX Core JPC-14 from the Alpha Ridge, Arctic Ocean

Yanwei Wang
Department of Earth Science
University of Bergen, Norway
November 2007

1. Introduction

1.1 The Arctic and in global climate change

The Arctic plays a significant role affecting global climate change. Present observations and climate models predict much greater warming in the Arctic region than the global average, which bring international attention to the region. In particular, there are concerns that melting sea ice and glaciers on Greenland/Canada may soon contribute to a substantial rise in sea levels worldwide (Smith & Millera et. al., 2003).

Increasing temperatures in the Arctic may cause large amounts of fresh meltwater to enter the North Atlantic, possibly disrupting global ocean current patterns and thus induce severe changes in the Earth's climate (Knies & Vogt, 2003).

Investigation of climate past uses records from ice sheets, tree rings, sediments and coral to map past state of the climate system on Earth. The Earth has undergone periodic climate shifts in the past, consisting of glacial periods separated by interglacial periods. This cyclicity is determined by the astronomical Milankovitch parameters (Berger & Loutre,2007).

Climate present and future can be understood by knowledge from climate past. One archive of the past climates is retained in Arctic Ocean sediments. In this thesis, I have studied magnetic properties of core JPC-14 from the Alpha Ridge in the Arctic Ocean, with the intension to extract information of climate variations.

1.2 Paleoclimate proxies and past Arctic Ocean circulation

Bischof & Darby (1997) studied data from the petrographic and geochemical analysis of ice-rafted debris (IRD) in the western Arctic Ocean. Provenance of IRD in four Arctic sediment cores implies that icebergs from the northwestern Laurentide ice sheets drifted across the western Arctic Ocean along the 180°- 0° meridian toward Fram Strait during the last 700,000 years. This ice drift was different from the present-day Beaufort Gyre circulation and indicates a different path of transpolar drift, implying climatic different conditions.

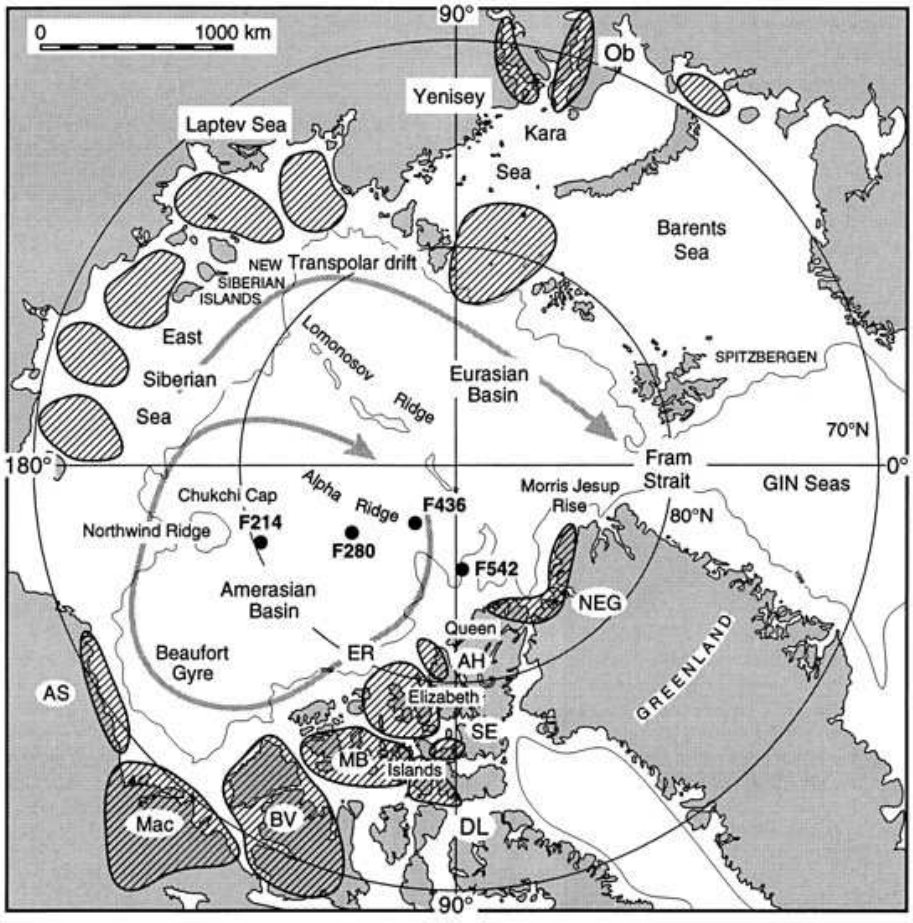

Fig. 1.1 Map of Arctic Ocean and adiacent landmasses with core locations and 1000-m isobath. Striped areas are source areas (Bischof and A.Darby, 1997).

1.3 Rock magnetic properties and chronology of Arctic sediments

We have studied rock magnetic parameters from a 12m-long core JPC-14, 149°02.041′W, 84°18.196′N, the water depth is1856m (Fig.1.3).

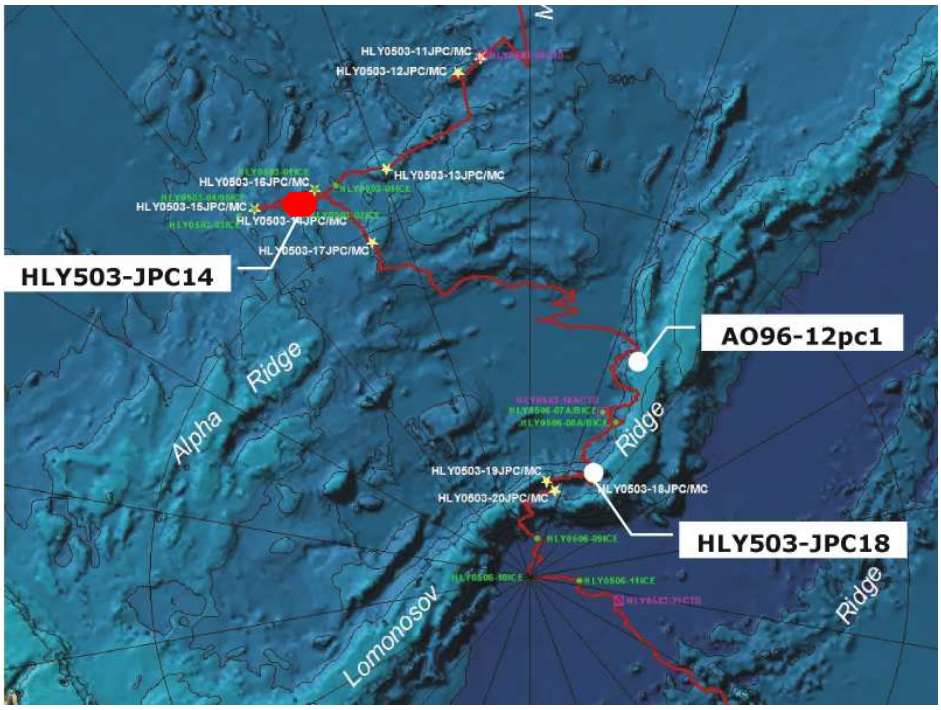

Fig.1.3 Bathymetric map of Central Arctic Ocean with the HOTRAX ship-trackand locations of the HLY0503 cores, the red circle is the site location of JPC-14.

It is well known that the rock magnetic properties of sediments cores , particularly magnetic susceptibility (MS), can be correlated with past climatic and oceanographic changes (Rousse, Kissel, et. al., 2006). Rock magnetic poperties have been studied in our lab, results of MS, thermomagnetic analysis (TMA), anhysteretic remanent magnetization (ARM), saturation isothermal remanent magnetization (SIRM) and S-ratios are shown in this thesis.

It has turned out to be very probematic to obtain a time frame of the Arctic Ocean sediment cores because of the barren of microfossils, which limits the possibility

of dating in the way of biostratigraphy and the marine isotope stages (MIS) as well.

Magnetic palarity stratigraphy has shown the presence of short intervals of magnetic revesal which is inferred to represent geomagnetic excursion (Jakobsson, Løvlie, et. al., 2001). However, with no independent time frame, excursions cannot be used for reliable dating.

The recent establishment of SINT-800 (Guyodo&Valet, 1999) is promising to apply relative paleointensity (RPI) of the geomagnetic field for constructing time frames in sediments. Applying RPI for dating requires certain magnetic limitations of rock magnetic properties. A relative uniformity of the magnetic grain size and mineralogy may result in a reliable RPI curve.

In this study, a RPI curve has been constructed from my core. Combined with FAD of E. Hulexyi (Backmann, 2007, pers.com), this RPI has correlated with SINT-800, an age-depth model of core JPC-14 is established.

2. Sample preparation

2.1 Sub- sampling

The whole core was 11.33 m long and was divided into 8 sections (Table 2.2.1).

Table 2.2.1 Summary of core sections and samples

Section	Length (m)	Depth (m)	Gap (m)	No
1	0.88	0-0.91		88
2	1.48	0.91-2.40		148
3	1.48	2.40-3.88		148
4	1.52	3.88-5.41	0.03	152
5	1.51	5.44-6.94	0.03	151
6	1.50	6.97-8.44		150
7	1.51	8.44-9.95	0.01	151
8	1.42	9.96-11.33		142
Total	11.26	11.33		1130

All 8 sections were cut into 1 cm-long sub-samples using a specially designed u – shape device. Samples were transferred into plastic cubic boxes (6.18 cm^3). All 1130 samples were stored at 4□ to prevent from drying.

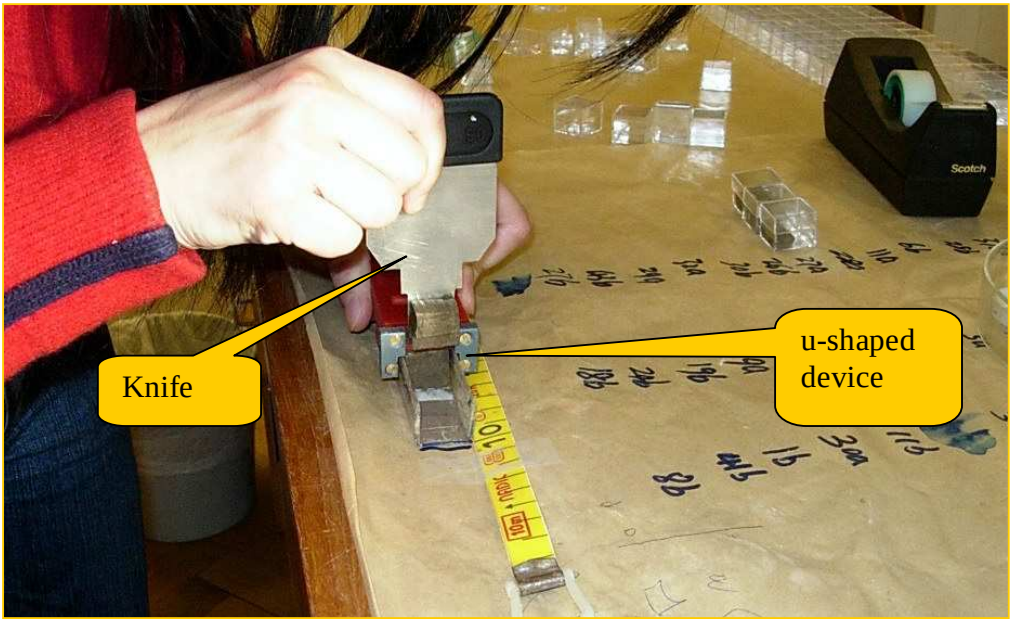

Fig. 2.1.1 Sub - sampling

2.2 Weight

The weight of each sub-sample was determined on an OHAUS GT410 electronic balance, using the weight-program Ohaus.exe.

Some sub-samples were less than 1-cm long and I used the weight to estimate the actual lenghth.

$$h_i = w_i / W$$

h_i – actual lenghth,
w_i – weight,
W – sum of all sub-samples in one section

3. Methods

Paleomagnetic methods have been applied to the samples (Løvlie &Walderhaug, 2003).

3.1 Magnetic susceptibility (MS)

Magnetic susceptibility (MS) is a fundamental parameter in paleomagnetic and rock/mineral magnetic investigations. It is a measure of the magnetization induced in a substance when exposed to a magnetic field. MS is defined by the ratio of the induced magnetization (J_{IND}) and the applied magnetic field (H):

$$MS = J_{IND}/H$$

Volume susceptibility (κ) is given as SI unit and the unit o mass specific susceptibility (χ) is m^3kg^{-1}.

3.1.1 Core Magnetic Susceptibility

Whole core Magnetic Susceptibility (WCMS) and Surface susceptibility (MS2E) were measured by a GeoTek Multi sensor core logger (MSCL) belonging to the University of Stockholm. The MSCL was installed onboard USCGC (US Coast Guard Ice-breaker) Healy.

The system was mounted in the Science Core Lab, and strapped to sustain movements of the ship.

The MSCL was equipped with the following sensors/units; gamma-density (^{137}Cs source), core-diameter, p-wave transducers and the 125mm in diameter whole core magnetic susceptibility (WCMS) loop for the MS2-unit.

WCMS were measured on USCGC Healy after coring out with a step of 1cm.

Surface susceptibility determination was done subsequently at the University of Stockholm at 0.5 cm intervals with a MS2E sensor.

3.1.2 MS at 77K and 293K

MS was measured at Liquid Nitrogen 77(K) and at room temperature (293K).

The method can give us information on magnetic grain size/domain state. Ferromagnetic, diamagnetic, paramagnetic minerals can all contribute to the MS. Diamagnetic MS does not change with temperature while paramagnetic MS changes according to the Curie law ($\chi \propto 1/T$). For magnetite, the MS may be constant or decrease about 80% at about 120K (Verwey transition).
SD magnetic grains have very low MS and do not change when cooled.
SP particles have high MS at room temperature. However, on cooling SP grains may pass the single domain boundary which results in a significant drop in MS. The relationship between the MS_{77K} and MS_{293K} can then show the different contributions of SP - grains in the samples.

If the ratio of MS_{77K}/MS_{293K} is less than 1, the sample is probably SP–grains dominated. Theoretically, the ratio can never larger than 3.83, since for a pure paramagnetic substance,

$$\chi_{77K} / \chi_{293K} = 293K/77K = 3.83.$$

The Kappabridge KLY-2 Magnetic susceptibility meter was used to measure the MS at the two temperatures (293K and 77K).

MS at 77K were measured quickly after being kept in Liquid Nitrogen for more than 15 minutes. 30 samples were put into a Dewar (2 L) filled with liquid Nitrogen for ca. 15 minutes. Samples were handled with a wooden clamp, transfering the cold samples from the Dewar into a styrofoam sample holder for measurement. All 1130 samples were measured in 20 days.

3.2 Thermomagnetic Analysis (TMA)
Thermomagnetic analysis may give valuable information about mineralogy. The Curie temperature (T_c) is the main parameter obtained from TMA. T_c is a critical temperature at which the spontaneous magnetization of a substance will disappear, and above the temperature, the substance will have paramagnetic

properties. The transition from a ferri-magnetic to paramagnetic state is termed a phase transition of the second order, which is thermomagnetically reversible.
The TMA method implies that a sample is heated to 700℃ or more in air or Argon atmosphere, various thermo-chemical induced alterations of the initial mineralogy may take place, such as, oxidation, inversion, creation of new magnetic phases and destruction of magnetic phases, which are the basis of the identification.
Different mineral has different T_c, which is independent on the amount of magnetic minerals.
The TMA was measured with an automatically recording horizontal translation Curie balance, which is controlled by a computer with the Curie program (5.0). All TMA measurements on HLY samples are heated in air atmosphere.
The gradient of temperature change is 20℃ /min, th e temperature range is 20-650℃, and the field was 6.02A, 725mT.

3.3 Anhysteretic remanent magnetization (ARM)
ARM is the the remanence produced during the smooth decay of a strong alternating field (AF) in the presence of a weak steady field (DC). It is generally imparted by subjecting a sample to a strong alternating field which is smoothely decreased to zero in the presence of a small steady field. It may be used for determining magnetic grain size of magnetite.

ARM increases in strength with the application of either a stronger steady field or a stronger alternating field until saturation is reached (Fig. 3.3.1). It is important to use an optimum field before imposing ARM on all samples.
For choosing a proper field, the following procedure was followed.

1. Use a field (AF) for which all samples have reached to ARM-saturation. In order to determine the minimum AF necessary to reach ARM-sauration, 20 samples based on three lithologic units were imposed ARM in varying

DC fields (0.25, 0.50, 0.75, 1.00G) and AF fields (25, 50, 75, 100, 125, 150, 200mT).

2. These samples are first imposed an ARM along the direction +Z, and then along the direction –Z in order to isolate an ARM unaffected by any remanences.

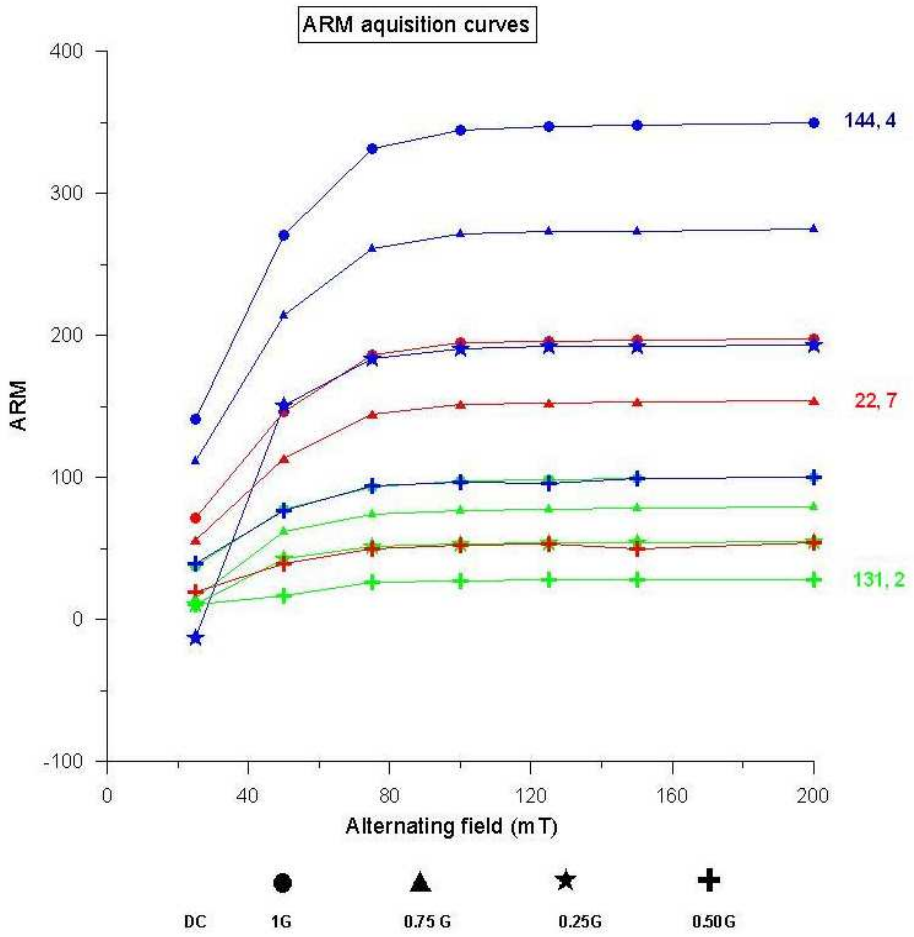

Fig. 3.3.1 Examples of ARM versus AC-fields and the DC-fields (the right: the numbers to sample no, section)

3. From the ARM acquisition curves above, in all DC fields, ARM saturated between AF fields of 75 to 100mT. The necessary ARM field was set be 100mT/1.0 G (See Fig. 3.3.1).

3.4 IRM-H Analysis

After ARM measurements, the samples were demagnetized in alternating fields 500 mT.

An IRM was imposed using a solenoid below 175 mT. Higher fields (maximum 4.5 T) were imposed in a Redcliffe Magtronics Pulse Magnetizer.
A Digico- spinner was used to measure the imposed magetisation.

For choosing an optimum saturation field, 30 new samples were selected from the lithologic units based on the WCMS curve together with ARM curve. These samples were first demagnetised after ARM measurement and then exposed to small fields initially (5mT), increasing to larger fields and eventually to the saturating field.

3.4.1 Saturation isothermal remanent magnetization (SIRM)

Saturation remanence (J_{rs}) is one of the main parameter derived from an IRM curve, known as SIRM. It is the strongest of the magnetic remanence that can be imposed in a sample by applying a large magnetic field. Measured on a mass specific basis, it is influenced by the concentration of all remanence carrying minerals in the sample. And the value is also strongly dependent upon the assemblage of mineral types and their magnetic grain size.

Remanent coercive force (H_{cr}) is another parameter extracted from IRM-H curves, it is the field (in opposite direction) which can bring saturation remanence J_{rs} back to zero.

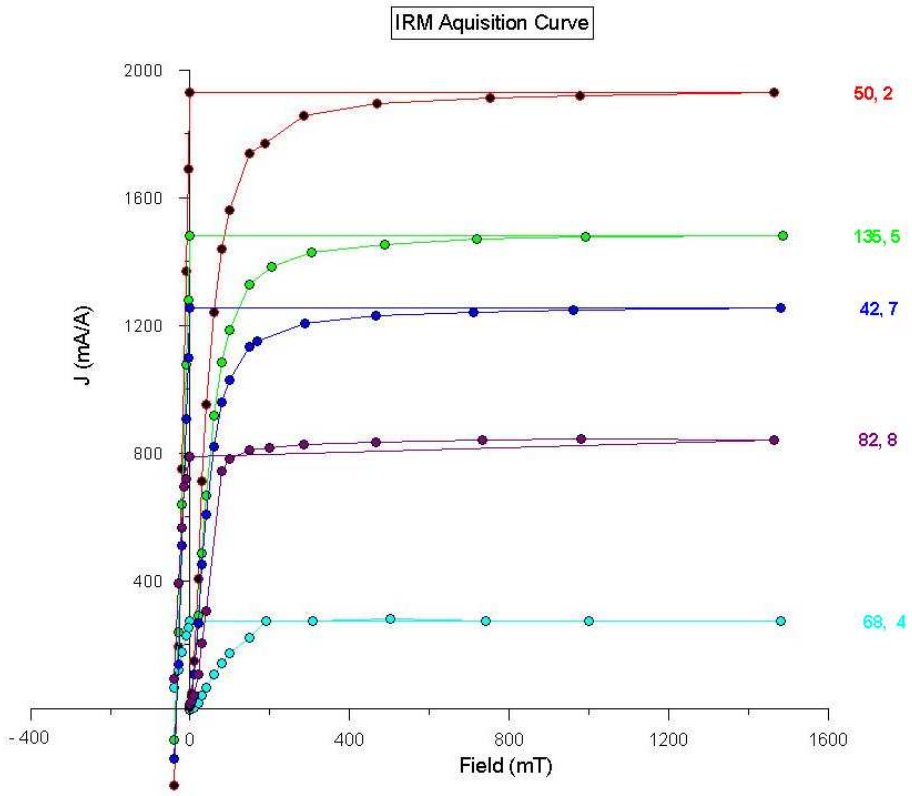

Fig. 3.4.1 IRM acquisition Curves (right: numbers of sample, section)

Based on the experiments on the selected samples, the saturating field was set as 1000 mT (Fig. 3.4.1).

Once saturated, the samples were exposed to two opposite fields, the so-called back-fields，100 mT and 300mT, in order to calculate the mineral diagnetic ratios of $S_{-0.1}$ and $S_{-0.3}$ parameters.

3.4.2 S-ratios

S-ratios are empirical parameters that are commonly used to discriminate between different magnetic minerals.

$$S_{-0.1} = IRM_{0.1T}/SIRM,$$
$$S_{-0.3} = IRM_{0.3T}/SIRM.$$

Different magnetic mineral aquire the greatest proportions of their remanence at different fields. Thus, ferromagnetic minerals such as magnetite and maghemite acquire a strong remanence in relatively low field strengths and all but the finest grains will have reached saturation before 200 mT. Given the relative ease with which ferrimagnetic minerals acquire remanence, they are often described as magnetically ‘soft’. While by contrast, canted antiferromagnetic minerals such as hematite, acquire the majority of remanence at higher fields, they are referred to as magnetically ‘hard’. These kind of ‘hard’ mineral can reach saturation in a field higher than 1 T.

Both S-ratios have a range from -1 to 1. As the majority of magnetite is fully saturated in a field of 100 mT, samples dominated by this sort of magnetic behaviour produce $S_{-0.1}$ very close to -1. In contrast, samples that contain some high coercivity minerals have higher S-ratios. For samples with relatively low concentration of ferrimagnetic minerals, the ratios will be more positive. In this report, the negative S-ratios are given by its positive values.

If $S_{-0.3}$ ranges between 0.98 to1.00, it implies pure magnetite/maghemite.
For $S_{-0.3T} < 0.98$, there must be some harder magnetic minerals present, and the usual guess is hematite or ironoxyhydroxides.

4. Results

4.1 Magnetic susceptibility (MS)

4.1.1 WCMS

Concentration dependent MS has been determined by three curves, WCMS, MS2E and MS_{boxes}.

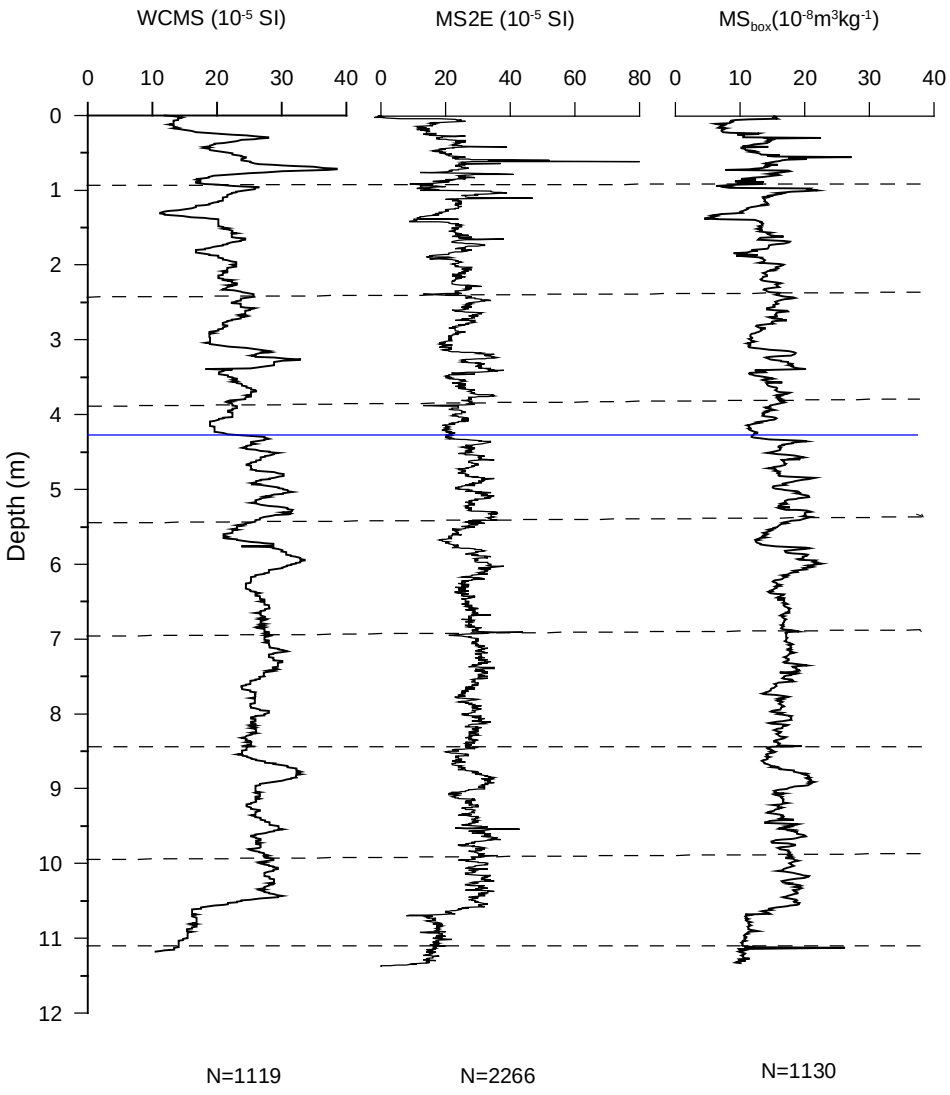

Fig. 4.1.1-1 Curves of WCMS, MS2E and MS_{boxes}. From left to right: lithomagnetic units based on the magnetic properties. The blue line marks the end of the conspicuous feature developed in all cores in the area. Note that below around 6.3m, the magnetic lithology shows small amplitude. Section boundaries are shown by horizontal dashed lines (the same as in other plots).

Look at the inspective curves above, the pattern of stratigraphic variations correlated well, except for an outlier at 11.13m appeared in the MS2E curve, which are also nerver seen in other seven cores records. It is most probably just noise.

The variability of magnetic susceptibility magnitude is little except for the largest peak appears in MS2E curve.

Distinct shipboard whole core magnetic susceptibility curve patterns records along 7 cores from the Alpha Ridge, among which there are two intervals with high conspicuous features.

One is the saw-shaped interval (feature d in Fig.6.2.1), the other is the massif-like interval around 8.5 to 9 m (feature e in Fig. 6.2.1).

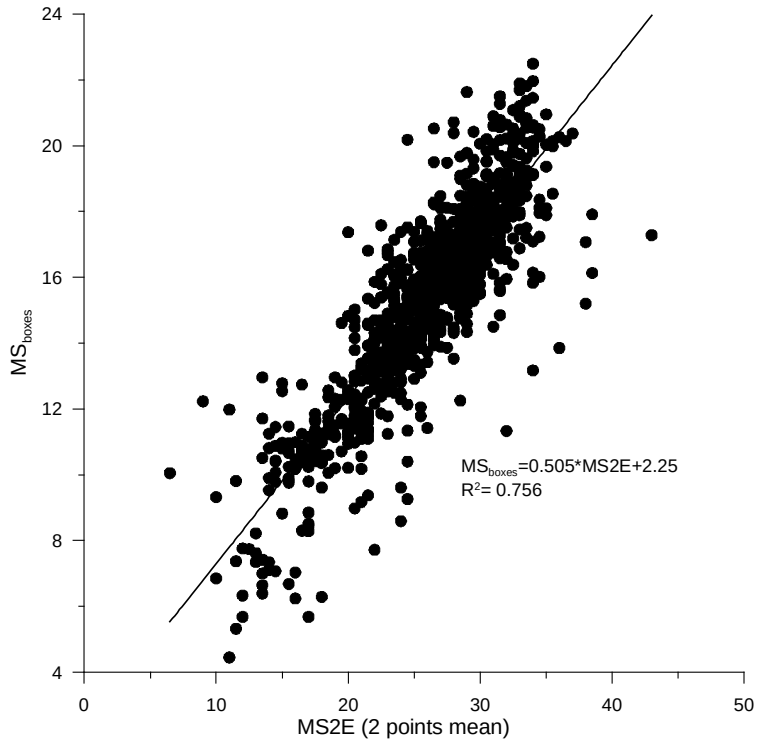

Fig 4.1.1-2 Scatter plot of MS2E (2-point mean) and MS_{Boxes}, 14 outliers.

Surface magnetic susceptibility MS2E was measured at a step of 0.5cm, while the length of box-sample was 1-cm. To make a feasible correlation of the two measurements, susceptibility of every two consecutive points were averaged to get a mean value to be correlated with the box-sample with the same depth.

Except for several scatted groups, the majority of the data points are limited to a linear relationship. The slope is a little large than 1, which indicates that the magnetic susceptibility measured one-centimeter long sample was a little higher than that measured along the surface in the same length of step. The good linear relationship shows both measurements are reliable.

4.1.2 MS at 77K and 293K

MS_{77K}, MS_{293K} and their ratios are plot together. Magnetic properties vary accordantly.

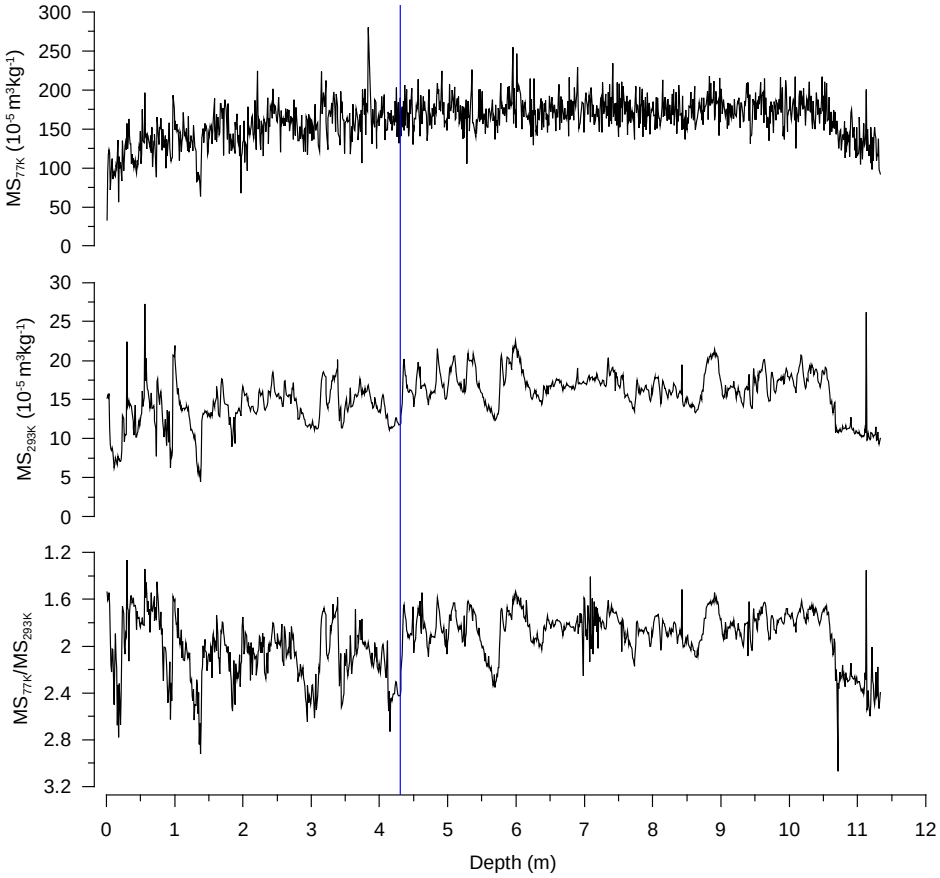

Fig 4.1.2 MS_{77K}, MS_{293K} and the ratio MS_{77K}/MS_{293K}. Note increasing MS_{77K}/MS_{293K} downwards. The vertical blue line marks sharp change in magnetic property.

The pattern of the former two curves are very similar, but because of the scale of MS_{LN} are 3 times of the MS_{RT}, the similar intervals are compressed, and the variation are not as apparent as seen in the MS_{RT}.

Showing in an opposite direction, MS_{77K}/MS_{293K} is consistent well with the former two curves. The higher the content of Magnetite, the lower the MS_{77K}/MS_{293K}, while the higher the MS, and the more paramagnetic minerals, the higher MS is.

4.2 ARM – ARM/MS

Three curves MS, ARM and ARM/MS. The horizontal blue line marks sharp change in magnetic properties.

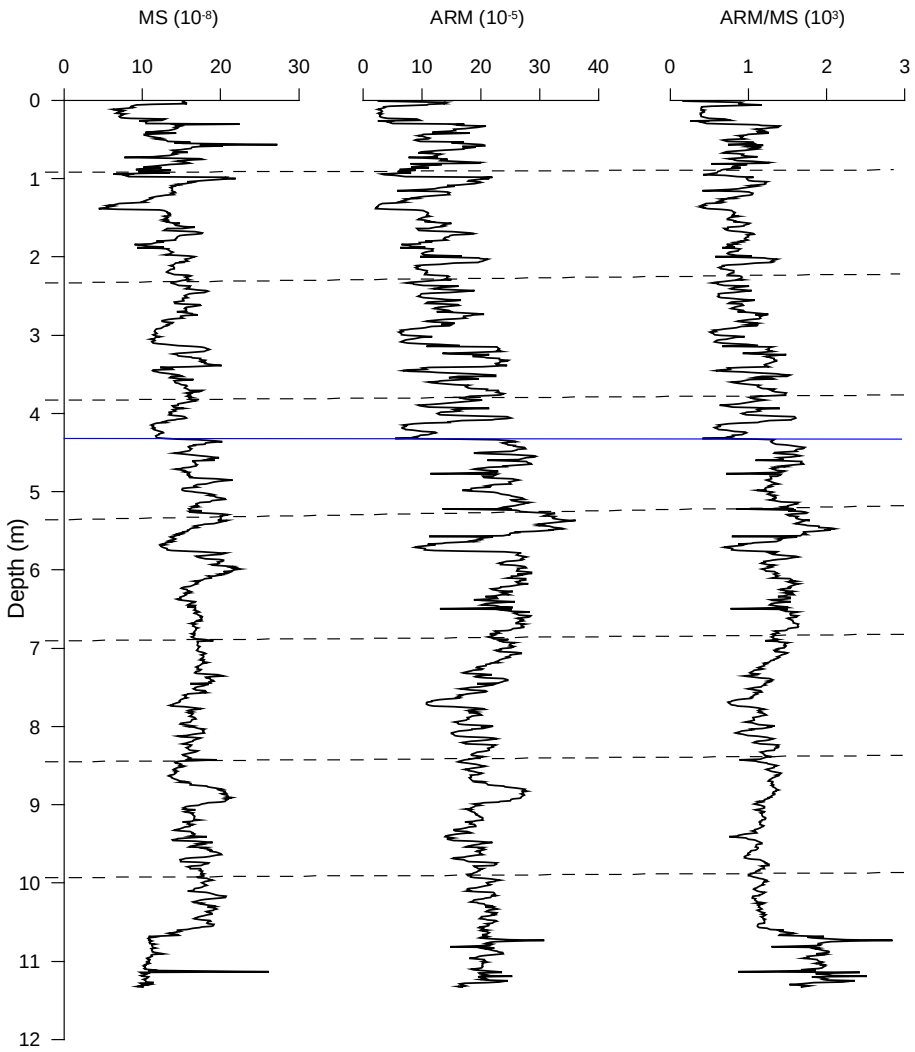

Fig 4.2-1 Curves of MS, ARM and their ratio, From left to right, there are curves of MS_{boxes} measured at room temperature, ARM and their ratios.

The MS_{boxes} show a slightly shallower trend from bottom to the top. Variation of magnitude is smaller at the bottom while relatively larger in the top (after the red marking line). Compared to the MS_{boxes}, the shallower from bottom to the top are slighter, and the magnitude of ARM are larger in the bottom while smaller in the

top. The variation of ratios follows the same trend as the MS curves, but the conspicuous massif-like interval at a depth around 9km is not obvious.

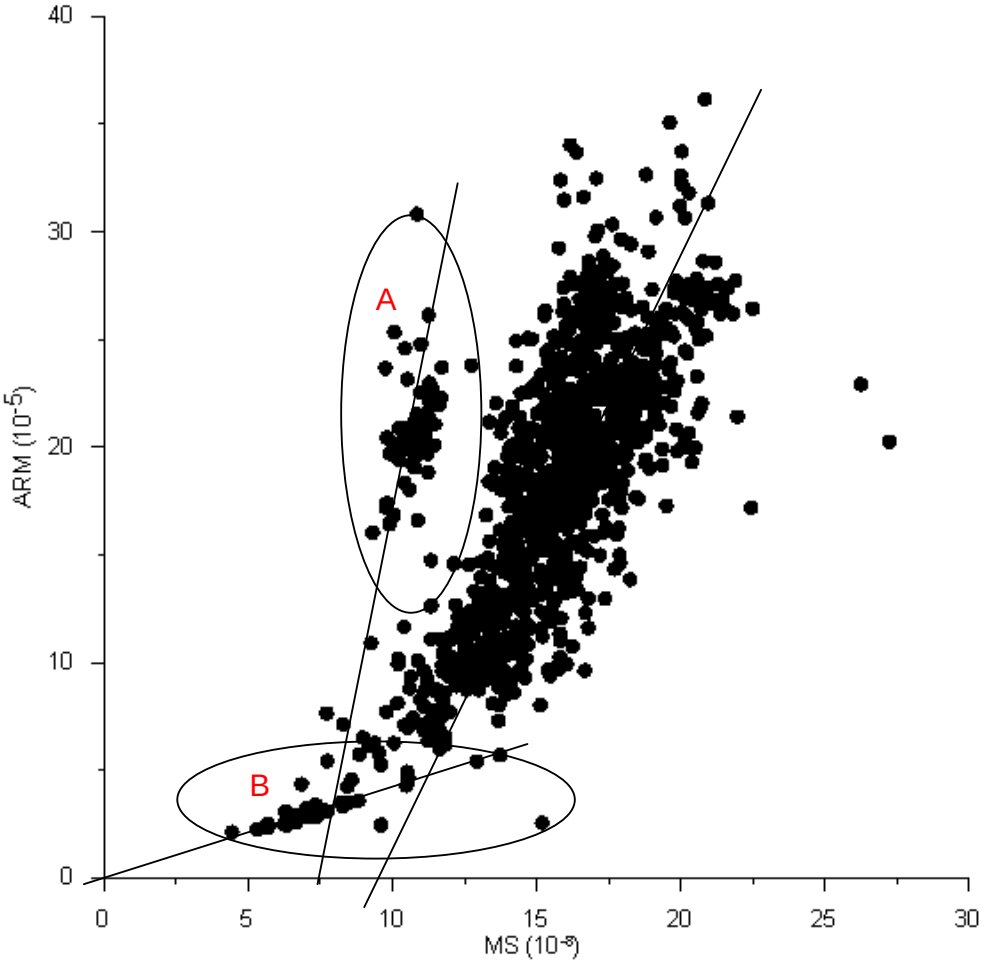

Fig 4.2-2 Curve of ARM and MS. Ellipse A represent a group with a higher ARM/MS ratio, which may be a finer mineral group. B represents the opposite group. The rest belong to the main group. Three regressive lines are drawn.

Compared to Fig. 4.2-1, it is easy to find group A is the oldest section along the core HLY-14, while group B is the younger section. The main group that goes along the same parabola is of middle age.

4.3 SIRM and S-ratios

MS_{boxes} measured at room temperature, SIRM and their ratios are plot together.

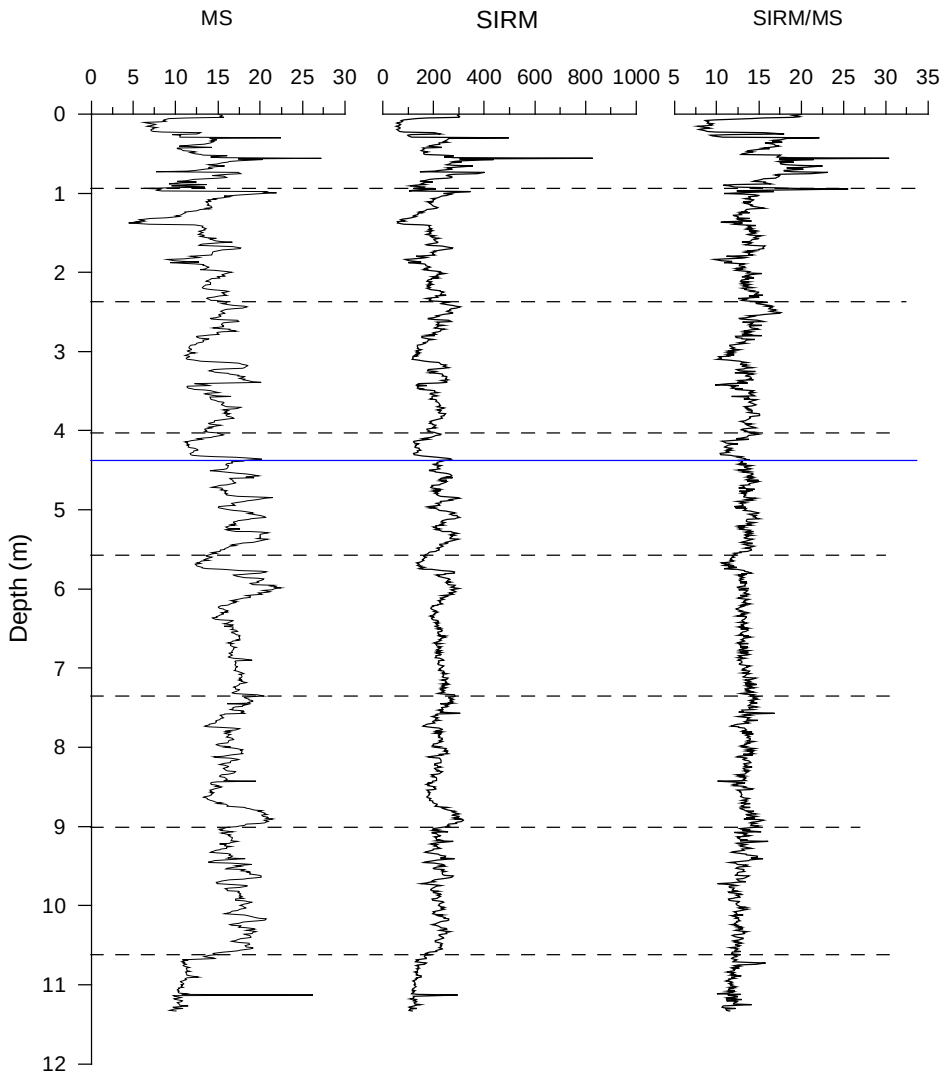

Fig 4.3-1. Curves of MS, SIRM and SIRM/MS. The horizontal blue line marks a sharp change in magnetic property.

Compared to the left MS curve, the SIRM show very slight variation from bottom to the depth of 2km. This larger variation on the top 2 kilometers is also shown on the SIRM/MS ratio curve. SIRM curve also clearly shows the two conspicuous

intervals (feature d & e in Fig.6.2.1) as in the MS curve, while they are not easily seen from the ratio curve because of the slight magnitude variation.

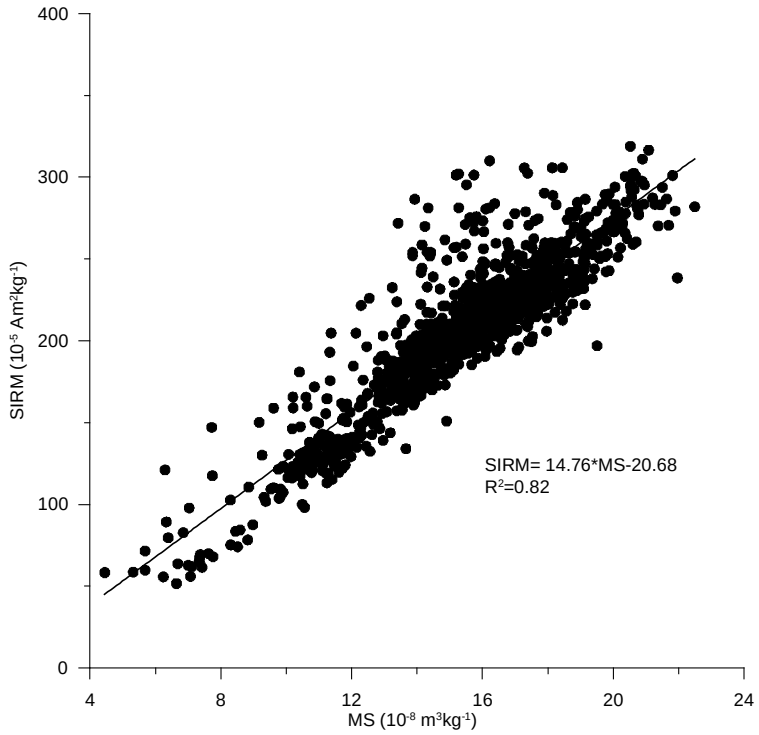

Fig. 4.3-2. Scatter plot of SIRM and $MS_{boxes.}$ Note: This linear relationship is expected. 7 outliers.

The plot shows a good linear relationship between the two measurements. These two parameters are both sensitive to coarser grains. The majority of data are concentrated, except for several scattered, deviate a little upwards or some downwards.

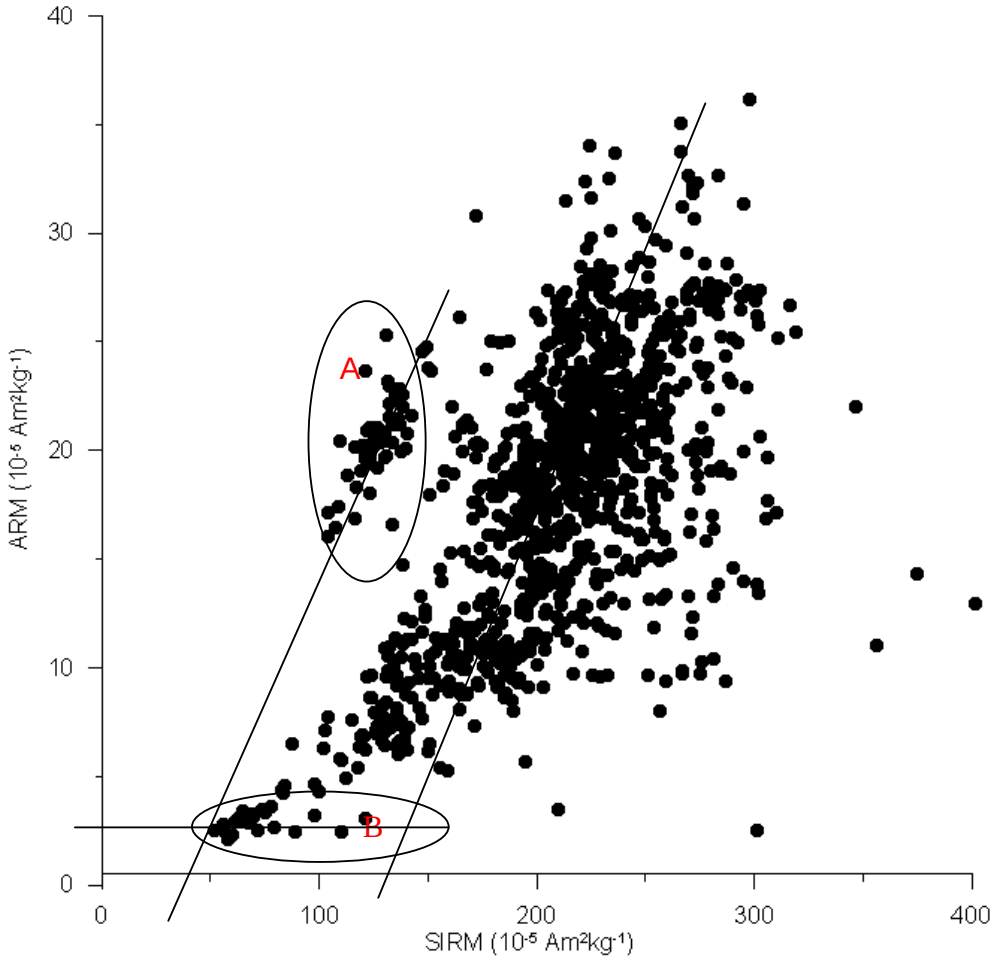

Fig.4.3-3 Scatter plot of SIRM and ARM. Note: The two ellipses groups should belong to the same section along the core HLY-14 as they are in the from the ARM/MS curve. Linear regressive lines of different groups are plot also.

4.4 S-ratios

SIRM curve is correlated with $S_{-0.1}$ and $S_{-0.3}$. The result is shown below.

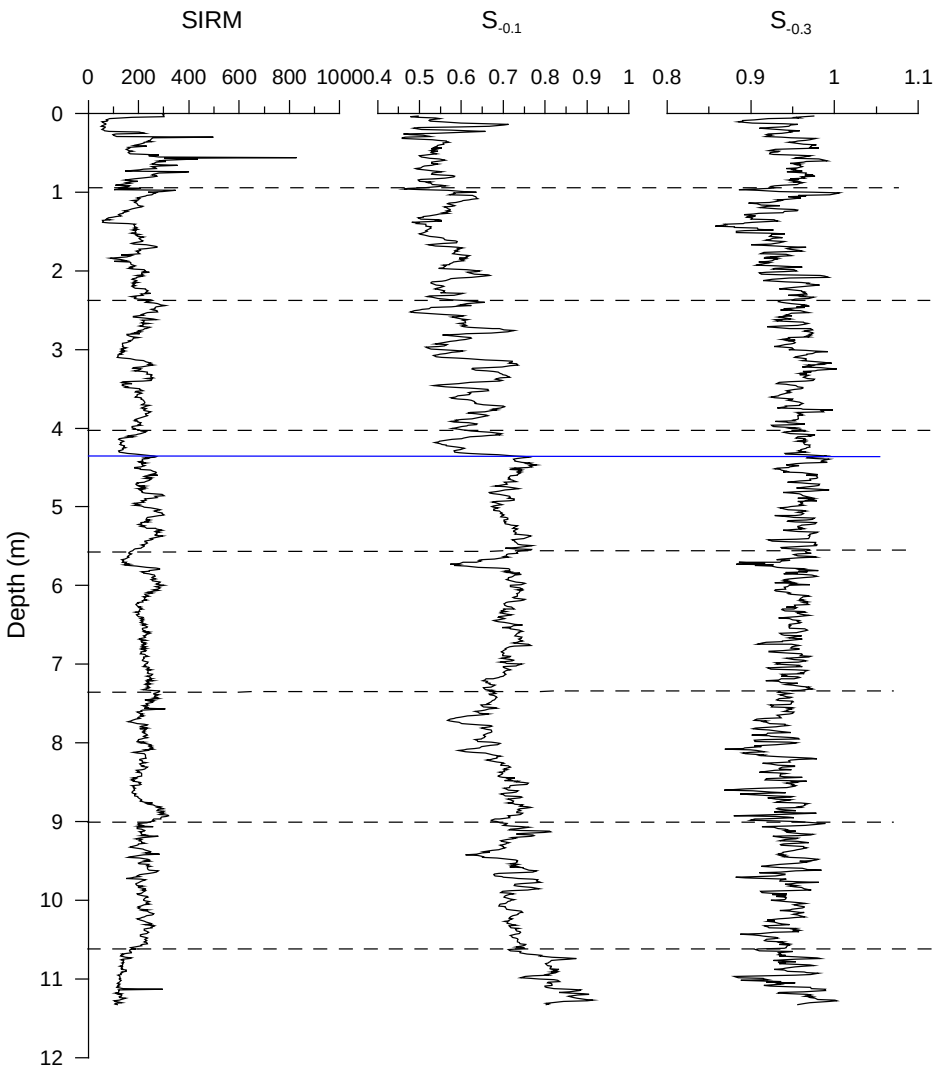

Fig.4.4 Curves of SIRM, $S_{-0.1}$ and $S_{-0.3}$. From left to right, there are curves of SIRM, $S_{-0.1}$ and $S_{-0.3}$, both two S-ratios are 3-point running data.
The horizontal blue line marks an abrupt change of $S_{-0.1}$, which can also be seen from the other two curves.

$S_{-0.1}$ curve show a more obvious variation compared to the $S_{-0.3}$ curve. There is a sharp decrease of $S_{-0.1}$ after the red dashed line, while the variation of $S_{-0.3}$ is very slight, which is confined to a range of 0.85 to 0.98, most larger than 0.90.

S ratios show relative soft magnetic minerals, combined with TMA curves above, magnetite or titanemagnetite may occupy a large fraction.

4.5 TMA

Curie temperature (T_c) and the spontaneous magnetisation (M_s) are all material constants. T_c is critical temperature. At this temperature, the spontaneous magnetisation of a substance will disappear, and above the temperature, the substance will have paramagnetic properties.

TMA method implies that if rock sample (very little) is heated to 700^0C or more in air or Argon, various thermo-chemical induced alterations of the initial mineralogy may take place, such as, oxidation, inversion, creation of new magnetic phases and destruction of magnetic phases, which are the base of the identification.

TMA curves are dried samples collected every 15 cm, heated in air, with a temperature increasing rate of 20 °C/min, in a field of 300-500mT.

Two types of TMA curves are typical in JPC-14 samples. Each counts up to half percent. Both curves have concave shapes, reflecting dominance of paramagnetism contributed. The baseline adjusted upward.

The two typical TMA curves of JPC-14 samples are shown below.

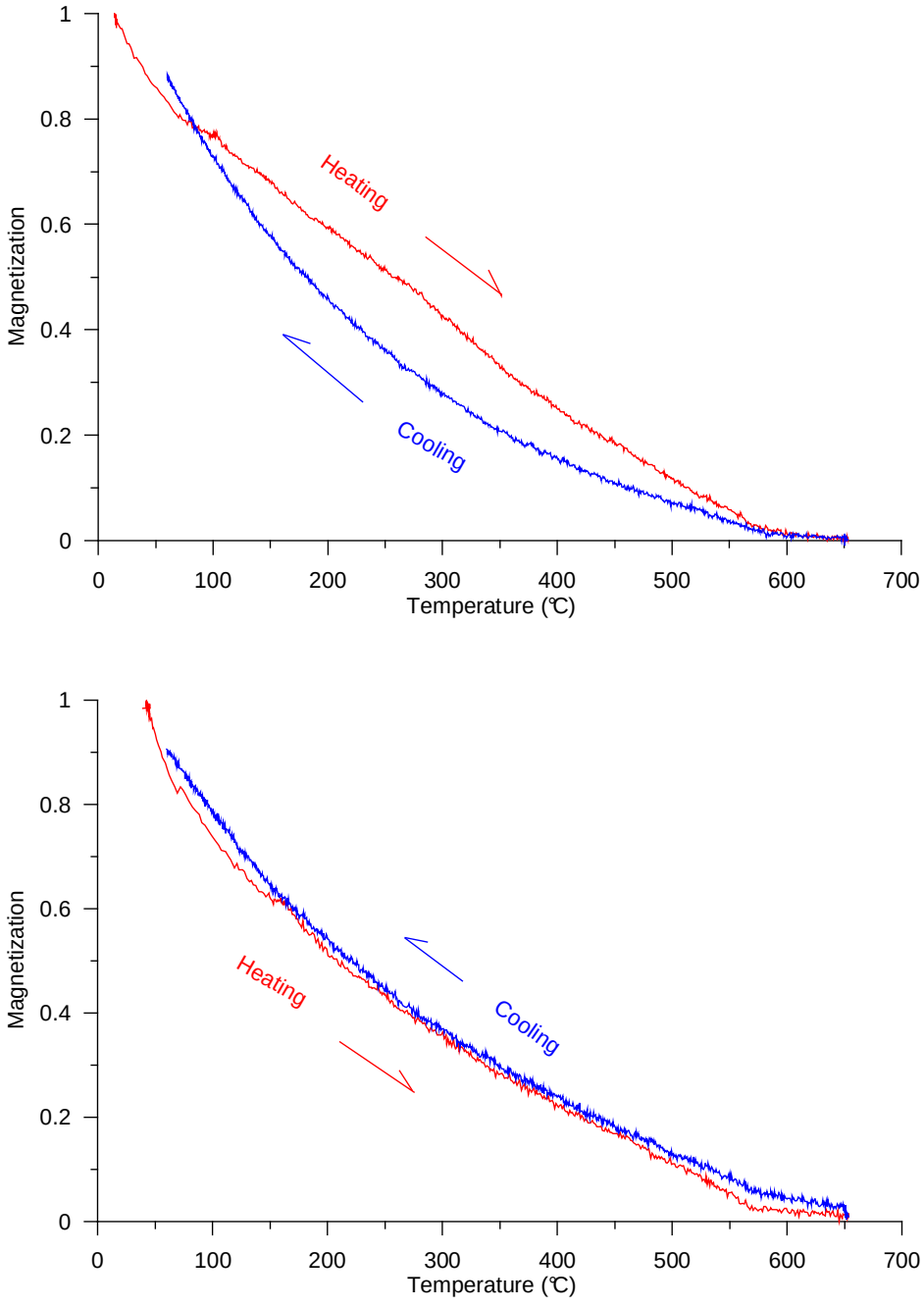

Fig. 4.5 High field magnetization variations with temperatures of sample JPC-14-1-54 (up) and JPC-14-5-52-0A (down).

The first type of TMA curve show a weak inflexion of maghemite on heating, a Tc of 570-580°C demonstrates a weak proportion of magnetite.
There is no discernable inflexion and a reversable Tc in the second type of TMA curve. Both of them show unusual low content of magnetite or maghemite in core JPC-14.

5. Chronology

5.1 Dating Arctic Ocean Sediment Cores

Marine sediments can be dated using biostratigraphy, oxygen isotope stratigraphy (marine isotope stage MIS) and magnetic polarity/excursion stratigraphy.

Biostratigraphy is based on fossil evidence contained in sediments. Strata from widespread locations containing the same fossil fauna and flora are correlatable in time. It is commonly demonstrated that a particular horizon in one geological sediment section represents the same period of time as another horizon at some other section carrying the same fossils. It is based on William Smith's 'principle of faunal succession'. A geologic time scale was developed acoording to this principle during the 1800s based on the observations of biologic stratigraphy and faunal successions.

Oxygen isotope stratigraphy is based on the oxygen isotope analysis on marine limestone sediments and ice cores. An oxygen molecule has three naturally occurring isotopes: ^{16}O, ^{17}O and ^{18}O. The most abundant is ^{16}O, with a small percentage of ^{18}O and even less ^{17}O. In standard mean ocean water (SMOW) the ratio of ^{18}O to ^{16}O is $2005 * 10^{-6}$. Fractionation occurs during changes between condensed and vapor phases: the vapor pressure of heavier isotopes is lower, so vapor contains relatively more of the lighter isotopes and when the vapor condenses the precipitation preferentially contains heavier isotopes. The difference from SMOW is expressed as $\delta^{18}O = 1000 * (({}^{18}O / {}^{16}O)_{SAMPLE} / ({}^{18}O / {}^{16}O)_{SMOW} - 1)$, δ values for precipitation are always negative (Brook, 2007).

Oxygen isotope analysis considers $\delta^{18}O$**,** the ratio of ^{18}O to ^{16}O. It is commonly used as a proxy of the temperature of precipitation, In paleosciences, foraminifera and ice core data ^{18}O:^{16}O is used as a proxy for temperature.

The $\delta^{18}O$ value of shells depend on the $\delta^{18}O$ in the surrounding water, which can be as variable as its temperature. This variability arises because when water

evaporates the lighter molecules of water holding ^{16}O tend to evaporate first, because of their lower mass. This makes the water vapor more depleted of ^{18}O than the ocean from which it evaporates. Similarly, when the temperature falls, the heavier water molecules will condense faster than the lighter water molecules. In glacial periods, more ^{18}O is trapped in ice, resulting in relative higher contents compared to most vaporized ^{16}O. The relative concentrations of the heavier isotopes in the condensate indicate the temperature of condensation at the time, allowing for ice cores to be used for global temperature reconstruction.

Arctic Ocean carbonate microfossiles are discontinuously produced and erratically preserved in sediments (Backman et.al., 2004). This lack of biogenic relicts sets limiations to the possiblity of dating northern high-latitude sediments in the way of biostratigraphy, and also the effectiveness of oxygen isotope stratigraphy (Matthiessen, Knies et. al., 2001). Paleomagnetic investigations have been applied to high-latitude cores during the past twenty years. A summary of the development of the application of magnetic- polarity are introduced.

Magnetic polarity/excursion stratigraphy is a chronostratigraphic technique using changes in the polarity of Earth's magnetic field. Modern developments of the Geomagnetic Polarity Time Scale (GPTS) was initiated in 1960s. In general, following advances in potassium-argon (K-Ar) dating of Pliocene-Pleistocene igneous rocks, igenous rocks with the same age but from widely separated localities were found to have the same paleomagnetic polarity. Age and magnetic polarity determinations of increasing numbers of igneous rocks were compiled and led to the establishment of geomagnetic time scale in the 0- to 5-Ma time interval. The GPTS has an upper limit of around 5 Ma because K-Ar dating has a precision of 1%, implying that to a measured age of 5 Ma, the uncertainty is 50 ka, which is larger than durations of some sub-chrons.

Geomagnetic excursions represent short-duration, high-amplitude directional changes of the geomagnetic field. The duration is of the order of 1 ka to 5 ka. There is yet no geomagnetic excursion time scale (GETS) established.

Sediments from northern high latitudes recorded steep negative inclinations. What we are interested to find is whether these negative records is due to geomagnetic variations throughout the Brunhes Chron or not. Recent synthesis of paleomagnetic high-frequency directional features of the field was published by Løvlie (1989a, b).

Dating Arctic Ocean sediments using paleomagnetic inclination data have been shown by Nowaczyk, who has successfully correlated magnetic inclination zones with established geomagnetic excursions. Investigations of two cores from the eastern slope of the Yermak Plateau (82º1.9¹&82º4.2¹) reveal convincing evidence for four polarity events, which are clearly documented with full reversals of the ChRM incliantions of the Earth's magnetic field during the last 170 ka (1994), high-resolution magnetostratigrapy were applied to sediments from the Arctic Ocean, and steep negative inclinations indicated evidence for the existence of the the Laschamp excursion (37-35ka), the Mono Lake excursion (27-25,5 ka) and possibly another very short excursion (22ka) (Nowaczyk, 2000).

Jakobsson et al. (2000) established sequential variations in Manganese Oxide (MnO) content and color of a deep-sea core retrieved from the Lomonosov Ridge (87ºN) in the central Arctic Ocean. Variations in MnO mimic global low-latitude $\delta^{18}O$ records, providing stratigraphic information that together with biostratigraphic data permitted the construction of a detailed chronological model (Fig. 5.1.1). Reidar and Jakobsson correlated $\delta^{18}O$ with the master polarity and with the Mangenese color respectively, the moment they sent theire own to the other, they found the perfect fit relationship does exist.
$\delta^{18}O$ minimum correlates with medium to dark brownish MnO layers, the lower the $\delta^{18}O$‰, the deeper the MnO color is, which may reflect the more oxidation

process once occurred. This in theory can be explained by the Arctic Ocean topography as a circular basin. During global colder stages, it was covered by ice, forming a reducing environment due to bio-assisted process reducing iron to Fe^{2+}. When temperature increases, the permernant ice cover partly melts and opens to air. Mangenese may then easily be oxidized to MnO. The Fe^{2+} layer together with the in-between brownish MnO layers are therefore most possibly modulated by climate.

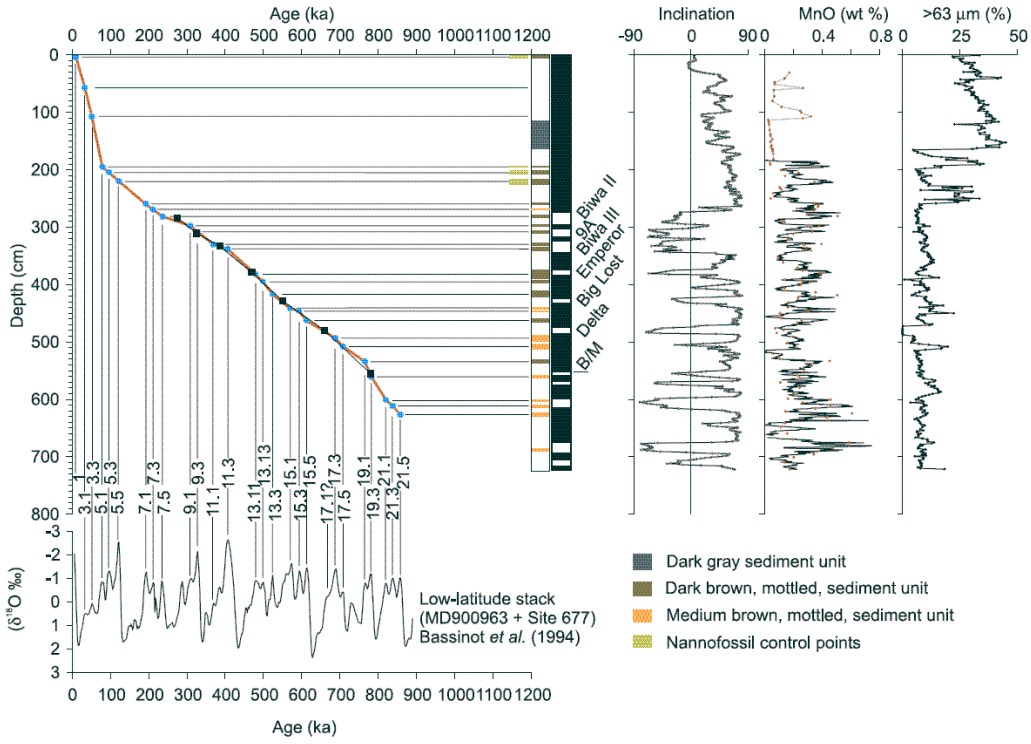

Fig. 5.1.1 Age model for core 96/12-1pc derived from nannofossil biostratigraphy and manganese and color cycles correlated to low-latitude $\delta^{18}O$ stack. Black boxes in age/depth plot represent Brunhes excursions, and blue filled circles represent manganese and color cycles correlated to oxygen isotope stages. Color cycles and names of geomagnetic excursions are indicated in two column on right side of age-depth plot. Red circles is the MnO content obtained from sub-samples, black line represents predicted MnO contents derived from red,green, and blue color values (Jakobsson et al., 2000).

5.2 Paleomagnetic data from JPC-14

Core JPC-14 was attempted dated using paleomagnetic properties. Complete paleomagnetic data sets were obtained from Løvlie. The Measurements were carried out in LSCE, Gif-sur-Yvette, France, measured by Catherine Kissel. Magnetic parameters NRM, ARM (0.05/100mT) and SIRM (1T) were measured on u-channels with an interval of 2cm.

Demagnetization was performed with static 3 axes alternating field (AF) demagnetization in fields of 5-10-15-20-30-40-50 mT on a cryogenic magnetometer (2G-750 DC).

5.2.1 Inclination of ChRM

The inclination of ChRM data was derived using the IAPD-program that uses least square method to find the best-fit lines and plane for directional data (See fig.5.2.1). A total of 600 measurement levels were analyzed. 'Mean Angular Deviation (MAD)' is used to assess the precision of the directional components (Krischvink J.L. 1980).

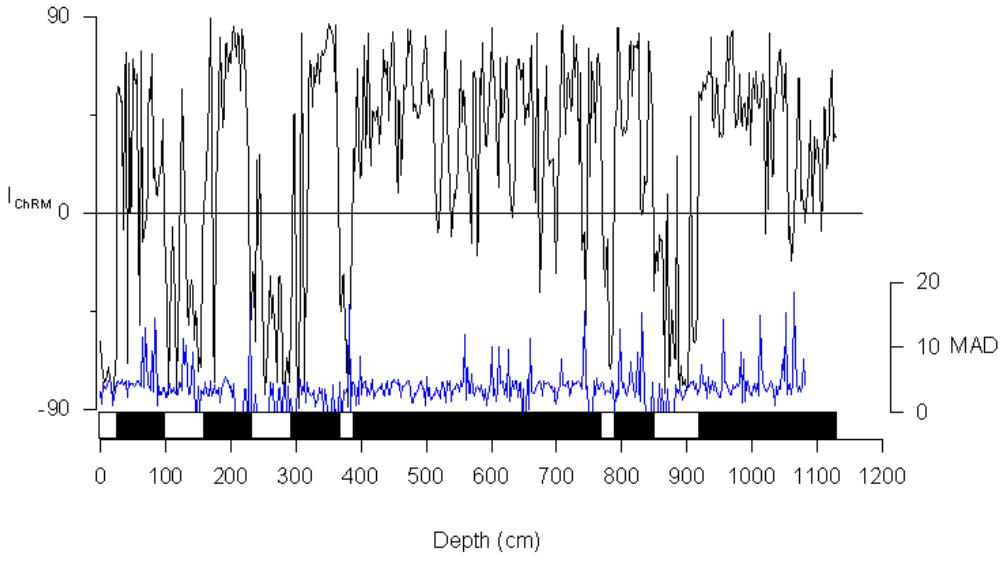

Fig. 5.2.1 ChRM inclination with inferred polarity reversals along JPC-14, together with MAD (blue line). Wherever the reverse peak is not very steep, there is usually a relative higher MAD, which indicates that the low amplitude negative peaks probably are artifacts of measurement.

The ChRM inclination defines several intervals with negative inclination during the assumed Brunhes normal polarity epoch. However, these intervals cannot be concluded to represent short-term polarity reversals because:

1. A zone with negative ChRM inclinations at the top of core JPC-14 is not a field configuration that is compatible with a recent geomagnetic field.
The reason for the negative inclination interval at the top could be due to:

a) the top is missing
b) erosion or non-deposition
c) artefact of coring
d) post-depositonal chemical alteration.

2. The mean sedmentation rate of JPC14 may be assumed to be 1.5 cm kyr^{-1} (according to results from other cores in central Arctic Ocean). If the indicated zones with negative inclinations are interpreted as excursions during the Brunhes normal polarity chron, most of the negative zones lasts longer than 10 ka, with some even 50 ka. This exceeds the duration of any known excursions (Butler, 1991).

5.2.2 MS and MS_{77K}/MS_{293K}

MS is a function of the sum of diamagnetic, paramagnetic and ferromagnetic contributions. Variations in MS can be regarded as reflecting variations in magnetic lithology. We have found some evidence for a correlation between Inclination transitions and MS variations.

The ratio MS_{77K}/MS_{293K} indicates the relative concentration of paramagnetic grains and magnetite. An upper limit of 3.83 represents the presence of only pure paramagnetic minerals. Decreasing ratios may be due to SP grains changing into SD grains on cooling to 77K or due to Verwey transition of magnetite at 118K. MS_{77K}/MS_{293} of box samples of JPC-14 show values below 3.83, which demonstrated there is Pseudo-Single-domain (PSD) to Multi-domain (MD)

ferromagnetic minerals dominated, no single-domain (SD) magnetic particles. Since MS_{77K}/MS_{293K} >> 1.0 (1.26-3.07, 90% ranged in 1.70 – 3.07), JPC-14 does probably carry SP-grains or significant amount of Verwey transition of magnetite. The ratio has higher amplitudes than MS. We also correlated the inclination with the MS_{77K}/MS_{293K}.

Inclination data is correlated to MS and the ratio of MS_{77K}/MS_{293K} (Fig.5.2.2).

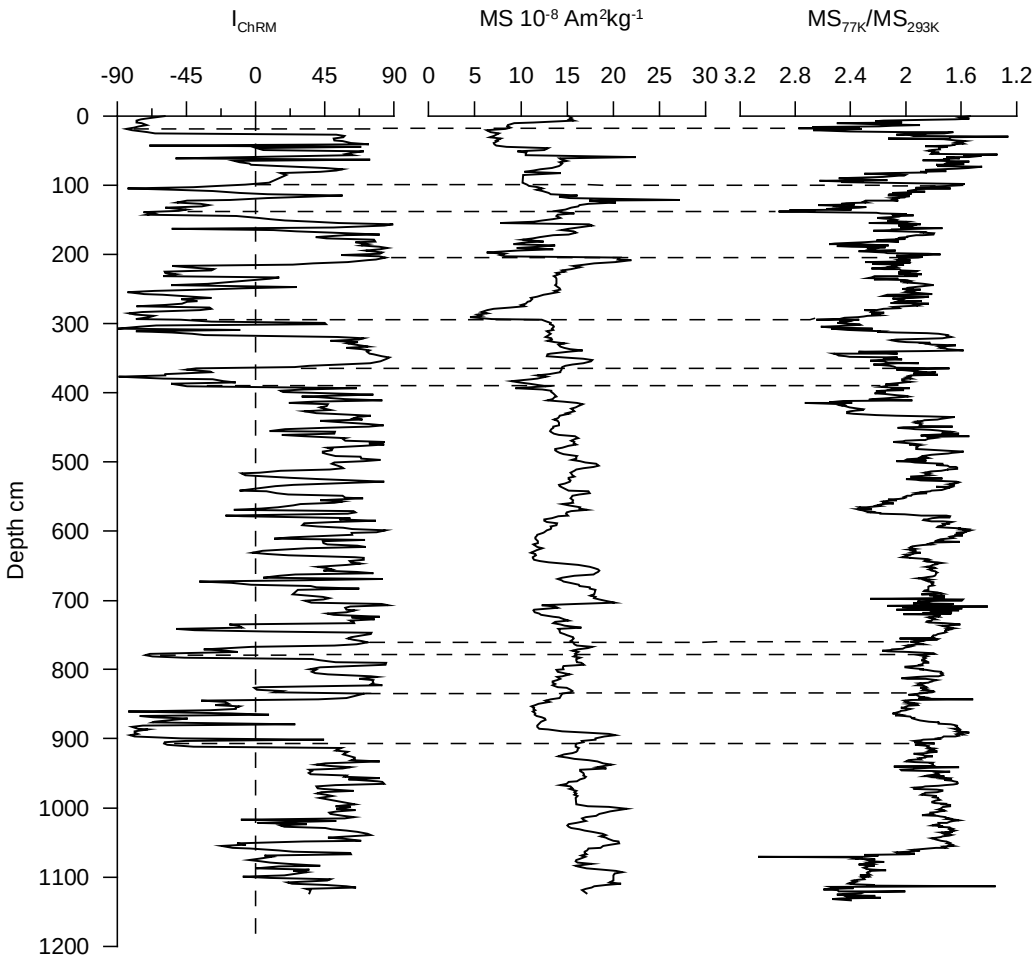

Fig. 5.2.2 ChRM inclination correlated with MS and MS_{77K}/MS_{293K} of core JPC-14. Dashed horizontal lines are transition boundaries of inclination

Correlated to the MS record, boundaries of inclination transitions, positive to negative or visa versa, appear to roughly coincide with the boundaries of lithology units infered from magnetic parameters (Fig.5.2.2).

Based on the inclination reversal boundaries, core JPC -14 has been divided into 12 inclination transition stages, named from the bottom and upwards as reversal stage 1, normal stage 1, reversal stage 2, normal stage 2 etc, ending at the top with reversal stage 6. Magnetic parameters are shown in a normalized depth, which is supposed to show the magnetic minerals developing with time during one polarity stage. Both u-channel and sub-sample data show good consistency. All curves in generally vary in accordant, but with small deviations between inclination-transition and lithomagnetic boundaries. This is because there are inevitable measurement shifts of the u-channel data. Here I just choose one parameter in different stages to show the magnetic property variation according to develop process (Fig. 5.2.3).

Most reversal stages (except for R3) start with a relative high ARM_{20mT}, and then decreases to a low ARM_{20mT}. If the stage is long enough, there will be another increase – decrease trend presents (see Fig. 5.2.3 (left)).
Note that the density of data points reflects the devloping extent of the sections. While the develop process during the normal stages show an opposite rule. Most Normal Stages (except for N2&N3) starts with a relative lower ARM_{20mT}, increases to a higher ARM_{20mT}. And also, in case of a longer stage, the cycle can be developed to repeat (see N4&N6).

Even the developing process does not seem exactly repeatable during each sub-divided stage, the intra-contrast did show similar trends among normal stage group or reversal stage group. It should be point out that the lithological properties are also affected by the sedimentation rate and the time it once spent. The faster the sediment deposited and the longer the stage lasted, the more variation cycles it was supposed to show. This process may provide a prove that the appeared inclination reverse is chemical-sourced. The longer time it endured, the developed the secondary chemical process.

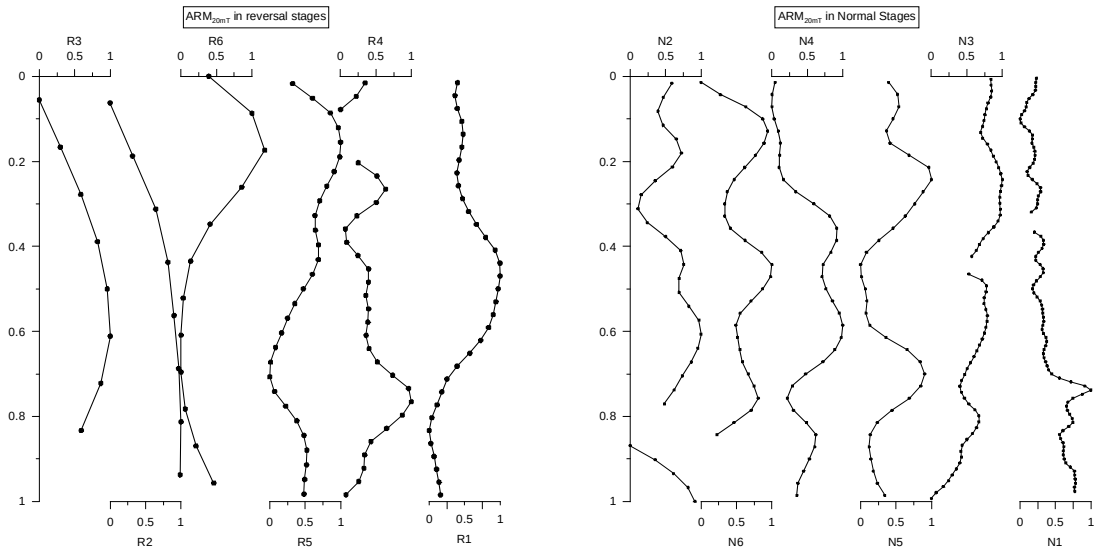

Fig. 5.2.3 ARM_{20mT} correlation plot in reversal (left) and normal stages (right). Note that they are shown according to developed thickness from left to right.

The appeared intervals of negative inclination are suggested to be unresolved remagnetization of chemical process. Theoretically, the appeared normal intervals may also be artifacts of CRM. However, it is rare for the CRM process in marine sediments (Sagnotti, Roberts et.al., 2005).

5.3 Relative Paleointensity (RPI)

5.3.1 Introduction

The basic assumption for retrieving relative paleointensity in marine sediments is that the remanent magnetization (NRM) intensity is a function of geomagnetic field strength. The NRM intensity is, however, also a function of the concentration of magnetic particles, the magnetic minerology and the alignment of magnetic grains.

Increasing concentration of magnetic minerals will result in increased NRM intensity. The alignment of magnetic grains may be both grain-size and shape dependent, as well as a function of compaction, bio-assistant processes.

Assuming that the degree of alignment of magnetic particles during deposition is proportional to the ambient magnetic field, numerous studies during the last decade have presented reconstructions of paleointensity variations of the geomagnetic field (e.g. Guyodo & Valet 1996, 1999). A relative paleointensity record from the Equtorial Pacific Ocean showed pronounced minima that were related tentatively by Valet & Meynadier (1993) to be short-term geomagnetic excursions within the Brunhes Chrons. The Ocean Drilling Program (ODP) has recovered many long sediments sequences from around the world that contain medium to high-resolution paleomagnetic records of Brunhes age. ODP paleomagnetic records and associated oxygen isotope chronostratigraphies have aslo greatly improved the understanding of the number and ages of Brunhes geomagnetic field excursions, and their relationship to normal directional secular variation and paleointensity variability (Lund, Stoner et. al., 2006).

Nowaczyk & Knies (2000) presented a new, and for the Arctic region exceptionally well-dated, high-resolution paleointensity record from 81.5ºN for the time interval 10-80 ka including the Laschamp polarity excursion at 37-35ka, the Mono Lake excursion at 27-25,5 ka, and possibly a short excursion at around 22ka.

χ_{ARM} is the Anhysteretic Susceptibiliry, which is ARM divided by the amplitude of the applied static field during its aquisition (1G in this paper) (King et al.1983). The ratios of χ_{ARM}/χ and ARM/SIRM can be used, as a first approximation, as indicating of relative grain-size changes with high (low) values indicating smaller (larger) particles (Fig 5.3.1-1).

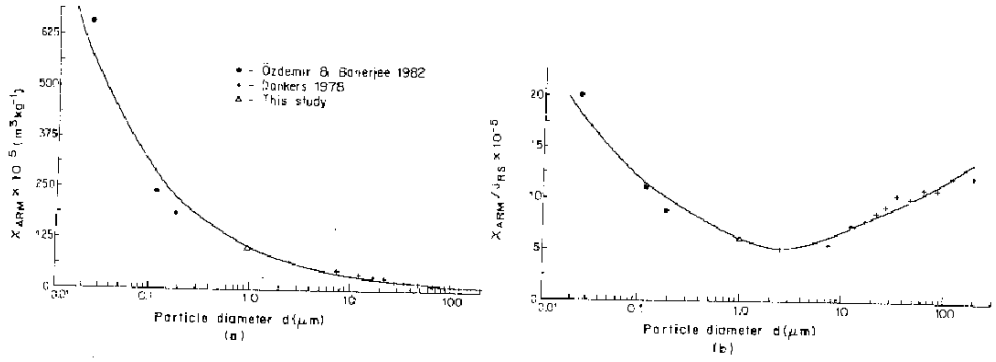

Fig. 5.3.1-3 (a) Partical size dependence of anhysteretic susceptibility (χ_{ARM}) for dispersed magnetites. (b) Particle size dependence of normalized χ_{ARM} for disperesed magnetites (King et al., 1983).

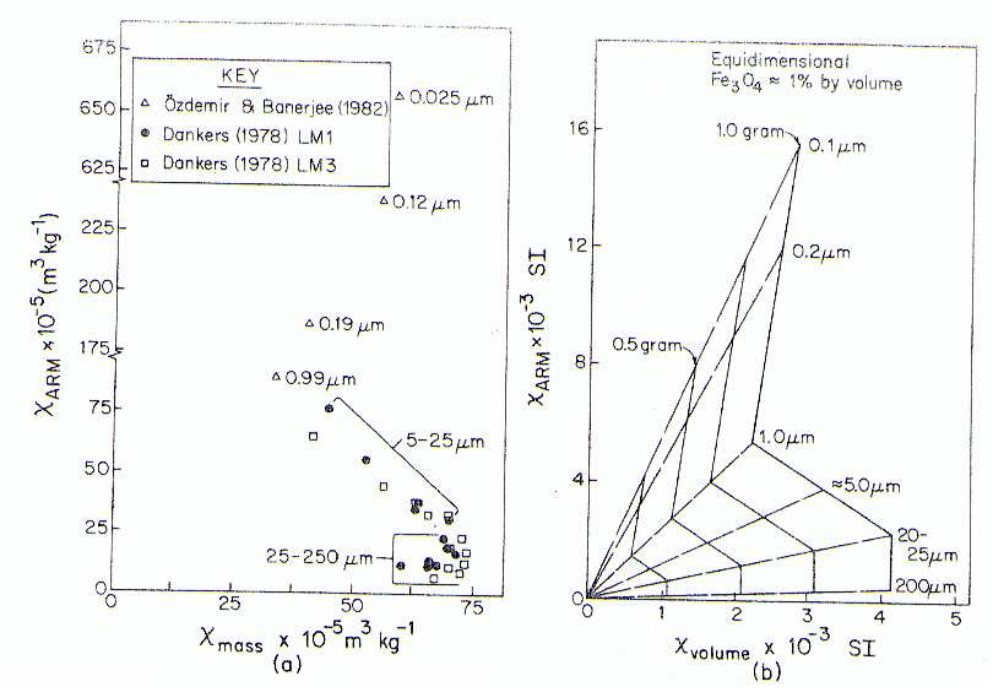

Fig.5.3.1-4 (a) Variation in χ_{ARM} versus χ (low field susceptibility) with particle size for dispersed equidimensional magnetite samples. (b) A simple variation in the magnetite content of natural materials (King et al., 1983).

Banerjee et al., (1981) discussed the potential for deriving a method for magnetic granulometry from the relationship between anhysteretic susceptibility (χ_{ARM}), which is particularly sensitive to SD and small PSD magnetite grains with low-field susceptibility (χ), which is more sensitive to the presence of coarser magnetite fraction (larger PSD and MD grains). Experimental verification of the potential use of the χ_{ARM} versus χ is shown in Fig. 5.3.4 (King et al., 1983). These data are from pure magnetite samples of known size and show continuous changes in the ratio of χ_{ARM} versus χ with particle size throughout the SD, PSD, and MD states.

To obtain RPI-curves, a proper normalization is required. By normalizing the NRM with respect to these magnetic parameters, the concentration dependent parameters such as MS, ARM, SIRM as well as grain-size variations can be eliminated. The signal linked to the geomagnetic field may be extracted.

Regarding the parameters related to the magnetic mineral concentration, MS, ARM and SIRM, the correlation of MS with SIRM yields a fairly linear trend (Fig. 4.4.1-2), whereas the correlation of MS with ARM is more scattered. There are several different populations of linear relationships (Fig.4.3.2).
The correlation coefficient of the ratios between ARM/MS and ARM/SIRM is 0.95, and 0.87 respectively.The scatter in the concentration dependent parameters are caused by grain-size variations, since ARM is mainly carried by smaller (single domain SD to pseudo-single domain PSD) magnetic particles, whereas MS and SIRM are linked more to larger (multidomain MD) particles.

Concentration- and grain-size-related rock magnetic parameters are plot together.

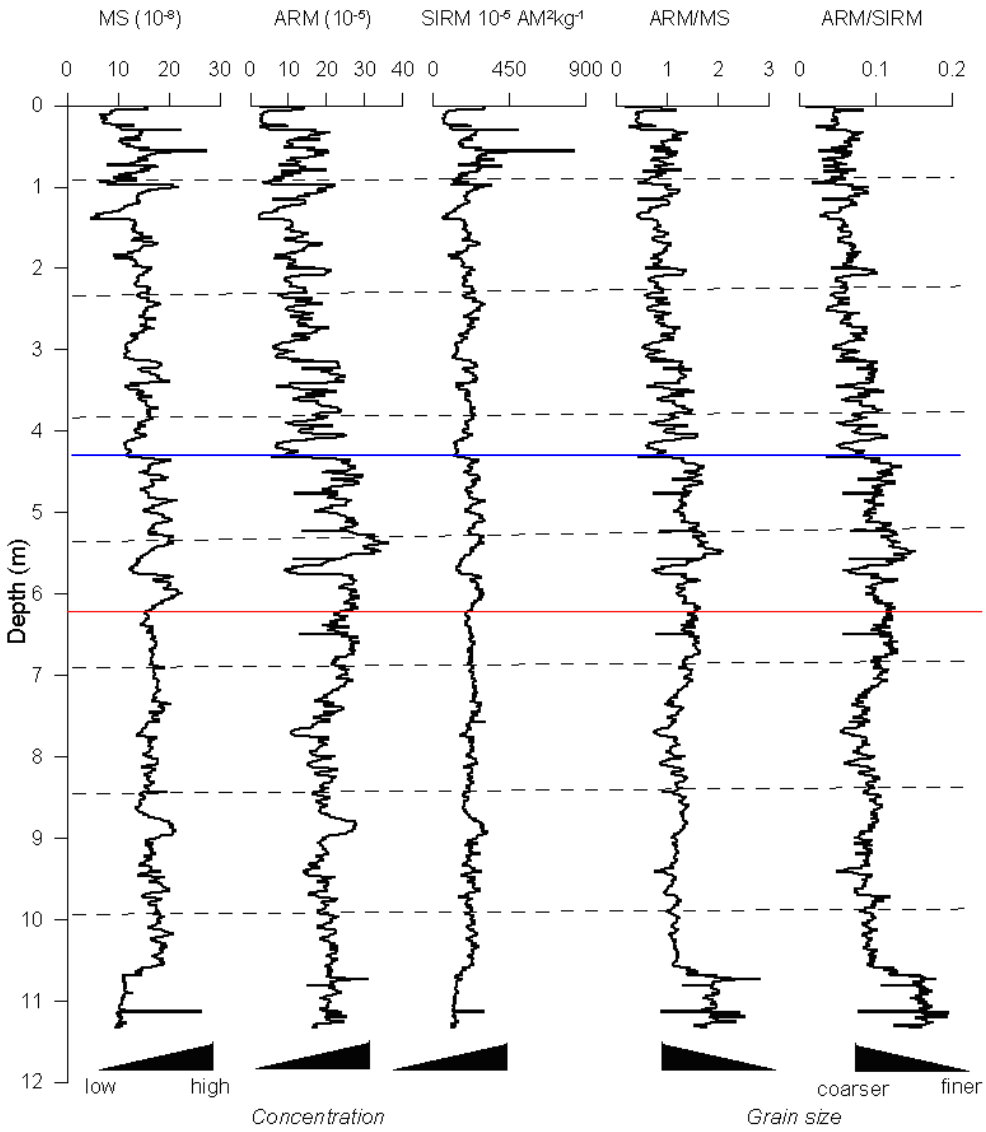

Fig. 5.3.1-1 Concentration- and grain-size-related rock magnetic parameters. Notice that below 6.3 m, each parameter declines to low amplitude, which is consistent with the red-line, below which marks a RPI-low. The horizontal blue line mark the sharp magnetic property variation.

Below around 630 cm, magnetic parameters vary but have very low amplitudes.

5.3.2 SINT-800

Recent advances in paleomagnetic and dating techniques have led to increasingly precise records of the relative intensity of the Earth's past magnetic field. The compilation and analysis of these records can provide important constraints on changes in global magnetic field intensity and therefore on the earth's geodynamo itself.

Independent records of relative magnetic paleointensity from sediment cores from different areas of the world have been stacked to extract a first order data set for the evolution of the geomagnetic dipole moment. So far, this procedure has been limited to the past two million years, and shows a fairly good agreement with absolute dipole moments derived from volcanic lavas.

SINT-800 (Guyodo &Valet 1999) is a stack of globally distributed relative paleointensity records from marine sediment cores that provide information regarding the evolution of the relative strength of the dipole field during the past 800 kyr.

5.3.3 FAD of E. Huxleyi

FAD of the calcareous nannofossil (coccolith) FAD of E. Huxleyi records occurs at 260ka worldwide (David et.al., 1997) and is found at around 4.68 km in core JPC-14. The deposition rate at the Alpha-Ridge is averaged 15 mm/ka, and the age of the core is estimated to be confined within the Brunhes Normal Polarity Chron according to the facts from other cores around. I have chosen SINT-800 to do a high-resolution correlation.

One characteristic of SINT-800 is that many intensity lows have occurred during the past 800 kyr. SINT-800 is constructed with a resolution of around 3-5 kyr. A simple condition for the occurrence of excursions is that the dipole field remains anomalously low so that non-dipole effects are dominant.

5.3.4. RPI from JPC-14 correlated with SINT-800

RPI from JPC-14 has been constructed by using ARM and SIRM as normalizing parameters. To reduce effects caused by post-depositional viscous magnetization, the RPI is based on partially AF demagnetization of NRM, ARM, SIRM. I have been adviced to use data after 20 mT demagnetization by Løvlie. Ratios of NRM_{20mT}/ARM_{20mT}, a comparison between NRM and ARM lost during demagnetized in an alter field of 20mT as well as $NRM_{20mT}/SIRM_{20mT}$ are derived.

King et al. (1983) referred to the concept of 'magnetic uniformity' based on the dominance of magnetite and the absense of significant changes in concentration and grain size with time.

Three requirements were proposed to define the uniformity of a sediment : (1) uniform mechanism of detrital remanent magnetization, (2) uniform magnetic minerology, and (3) uniform magnetic particle size. To match these requirements, they also introduced methods to verify whether the sediment meet the requirments or not.

Magnetic parameters MS, ARM, $IRM_{-100mT}/SIRM$ together with $IRM_{-300mT}/SIRM$ measured on 1-cm samples confirm the uniformity of magnetic minerology and magnetic particle size of core JPC14 (see Fig. 4.1.2, Fig. 4.3.1 and Fig.4.4.2). The magnitude of concentration dependent parameters MS, ARM and SIRM confines within a narrow range, and S-ratios also show little variation with depth.

The values of NRM_{20mT}/ARM_{20mT} and $NRM_{20mT}/SIRM_{20mT}$ are relatively low. They were both normalized with respect to their mean values, and the average of the two corresponding ratios are interpreted as the RPI index of the geomagnetic field.

Assuming that the obtained RPI for JPC-14 is a genuine continous record of geomagnetic field intensity variation, this RPI-curve has been correlated to SINT-800. Dated to 260ka worldwide, FAD of coccolith E. Huxleyi is found at a depth

of 4.68m in core JPC-14. Using this depth as a fixed chronostatigraphy tie-line, RPI is attempted to be correlated with the SINT-800 intensity curve based on the relative intensity variation (see Fig. 5.3.4-1).

The relative weak signal of RPI from feature points 11 (around 630 cm) to the end is noticed, which is consistent with other magnetic parameters shown in Chapter 4. This sharp decrease may represent variation in lithomagnetic mineralogy, which may reflect large changes of depositional environment. This depth is also the end of the widely developed conspicuous features on all six cores in the Arctic Ocean in core JPC-14.

The correlation has been done from both sides of the FAD of E. Huxleyi (vertical dashed line). Some features correlate very well (1,2,7,8,9, 10), while there are also some features that appear to be compressed (3,4,5,13) or expanded (6) (Fig. 5.3.4-1). Compress may due to erosion or lower sedimentation rate, while expansion may due to periods with faster sedimentation rates.

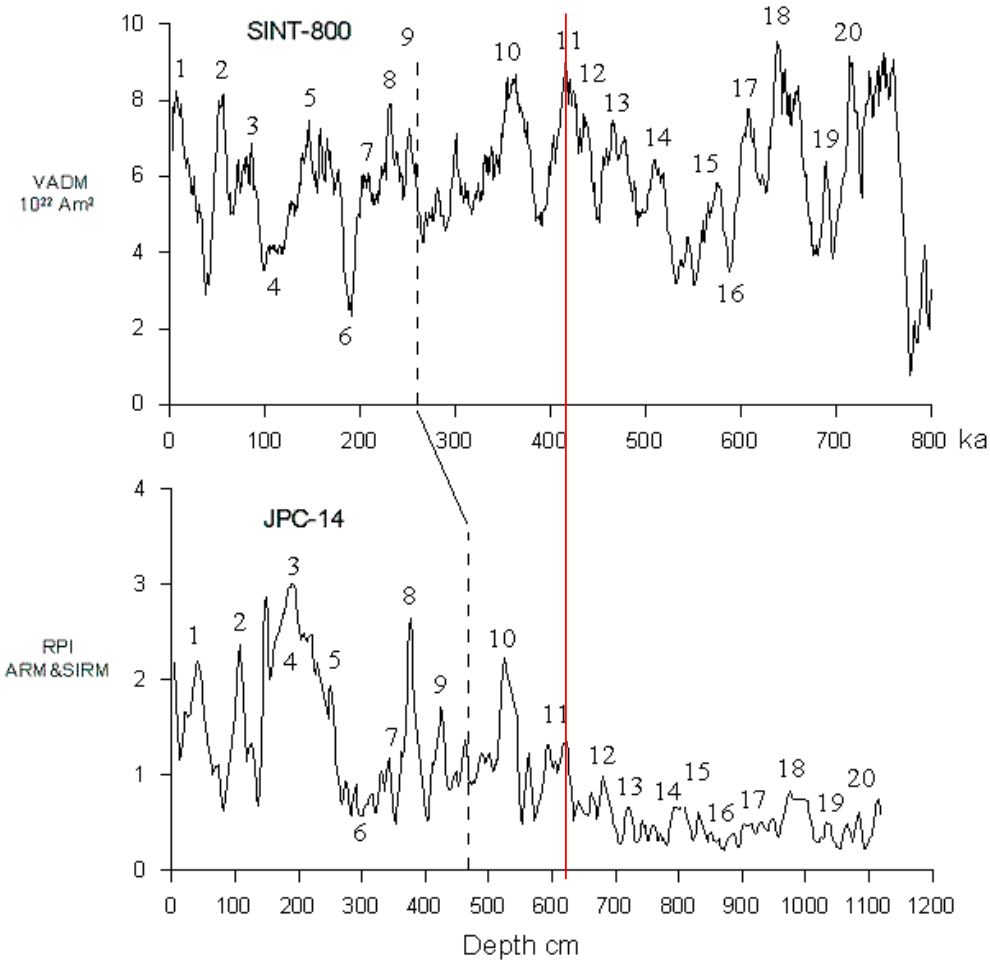

Fig. 5.3.4-1 Suggested correlation features between RPI JPC-14 and SINT-800. The feature points are indicated by numbers 1, 2, …20 etc. Dashed vertical line: FAD of E. Huxleyi (260ka). The vertical red line marks RPI low.

Based on the correlation, sedimentation rates between two adjacent feature points have been calculated and a continuous age-depth model is established (see Fig. 5.3.4-2).

This depth-time correlation is assumed to be genuine, and the following analysis of my data is based on this time-frame.

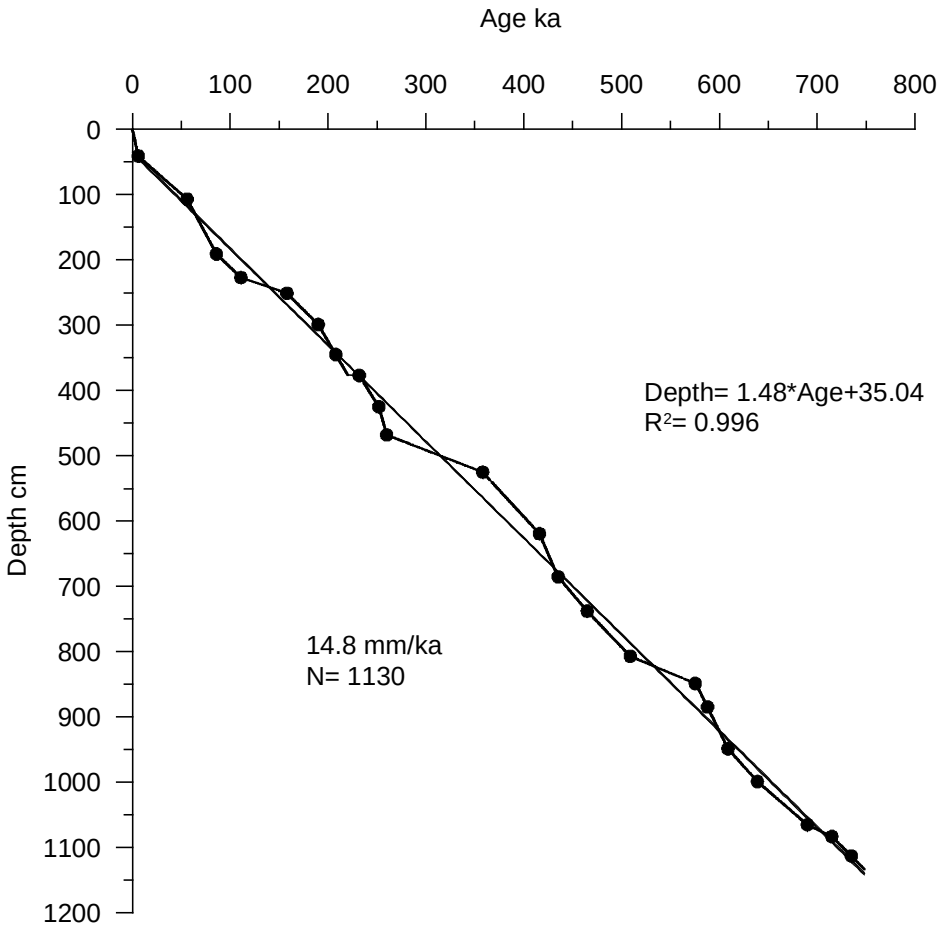

Fig. 5.3.4-2 Age – depth model defined by correlating RPI with SINT-800.

5.3.5 Inclination transition boundaries correlated with MIS records

The composite figure below shows that there is a pretty good fit between MIS boundaries and inclination reversal down to MIS 7.5, and RPI fits well with SINT-800. Except for MIS1, the miss fit may be due to erosion of the top of the core. During MIS 8 to MIS 12, ChRM is dominated by positive inclinations. From MIS 13 to MIS 15, the two boundaries again appear to correlate well.

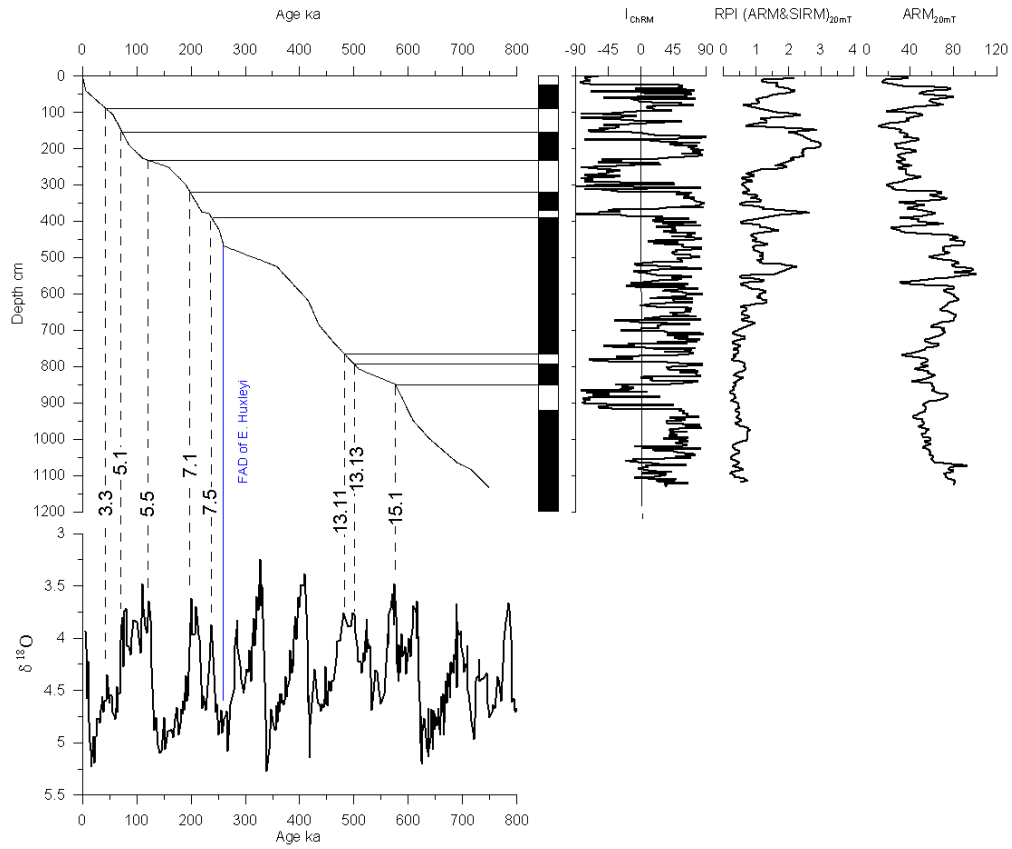

Fig. 5.3.5-1. Age model for core JPC-14 derived from RPI correlated with SINT-800 and FAD of E. Huxleyi (vertical blue line) correlated to ODP-677 $\delta^{18}O$ stack. Horizontal solid lines represent depth where Inclination are reversed, vertical dashed lines represent MIS boundary, different stages are shown by the numbers on the lines. RPI and ARM_{20mT} variations are indicated in two column on right side of age-depth plot. Note: ARM_{20mT} is shown in a inverse scale.

To express precise correlation before FAD of E. Huxleyi, the expanded plot down to 300 ka are shown below.

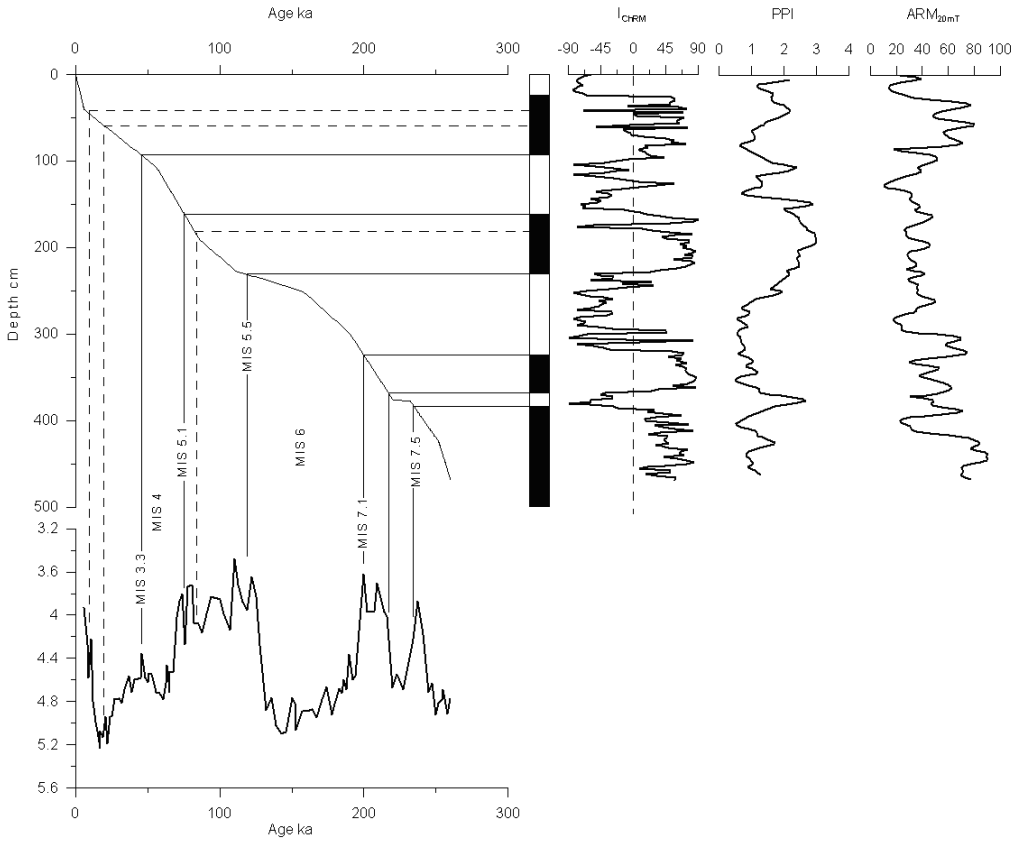

Fig. 5.3.5-2 Expanded plot from previous Fig. 5.3.5-1, covering time interval of 0-300 ka (same legend as fig.5.3.5-2).

Correlated $\delta^{18}O$ with the reversed inclination boundary, there is a link between glaciation and negative inclination, especially above the FAD of E. Huxleyi (4.68 km) (see Fig. 5.3.5-2). The intervals of negative inclination are not always following with RPI low, while the synchronicity of RPI lows with paleomagnetic excursions or events have been suggested by Thouveny, Carcaillet et. al.,(2004).

Both of these suspected that the appeared inclination reversals are most probably nothing to do with the geomagnetic field, but chemical driven artifacts in the rock magnetic parameters.

Sedimentation rates increase during glaciations. The relative long durations of reversed polarity intervals in cores from the Arctic Ocean suggests a link between glaciations and field reversals. The proposed mechanism for field reversals is the acceleration of the Earth's rotation, caused by lowering of the sea level during glaciations, and the short duration of events may implies that the geomagnetic field can reverse an order of magnitude faster than commonly assumed (Worm, 1997).

5.3.6. Mean sedimentation rates during MIS stages

According to the RPI-SINT 800 correlation, the mean sedimentation rates of different MIS stages can be calculated. The result is presented in table 5.3.6-1.

Table 5.3.6-1 Sedimentation Rates within marine isotope stages for core JPC-14

MIS	Depth in JPC-14 (cm)	Thickness (cm)	Age (ka)	Duration (ka)	SR (cm/ka)
1	49	49	12	12	4.08
2	49-65	16	12-24	12	1.33
3	65-116	51	24-59	35	1.46
4	116-158	42	59-74	15	2.8
5	158-237	79	74-130	56	1.41
6	237-299	62	130-190	60	1.03
7	299-399	100	190-241	51	1.96
8	399-498	99	241-312	71	1.39
9	498-512	14	312-335	23	0.61
10	512-564	52	335-382	47	1.11
11	564-619	55	382-416	34	1.62
12	619-740	121	416-466	50	2.42
13	740-820	80	466-530	64	1.25
14	820-839	19	530-559	29	0.66
15	839-968	129	559-620	61	2.11
16	968-1043	75	620-673	53	1.42
17	1043-1081	38	673-712	39	0.97
18	1081-				

SR= Sedimentation Rate (averaged during a certain stage)
Pink/blue= interglacial/glacial.

The fastest sedimentation rate (4.08 cm kyr $^{-1}$) appears during the first warm period, from 12 kyr ago to present (table 5.3.6-1). This is most probably erroneous because the top of the core may have been eroded, that means the interpreted age ‘zero’ at the top may be too young. The results show relative

faster sedimentation rates during most integlacial periods, while slower rates during glacial periods. Expections are found for MIS 4, MIS10 and MIS 12, where extremely high sedimentation rates are observed (see Fig.5.3.6-1).

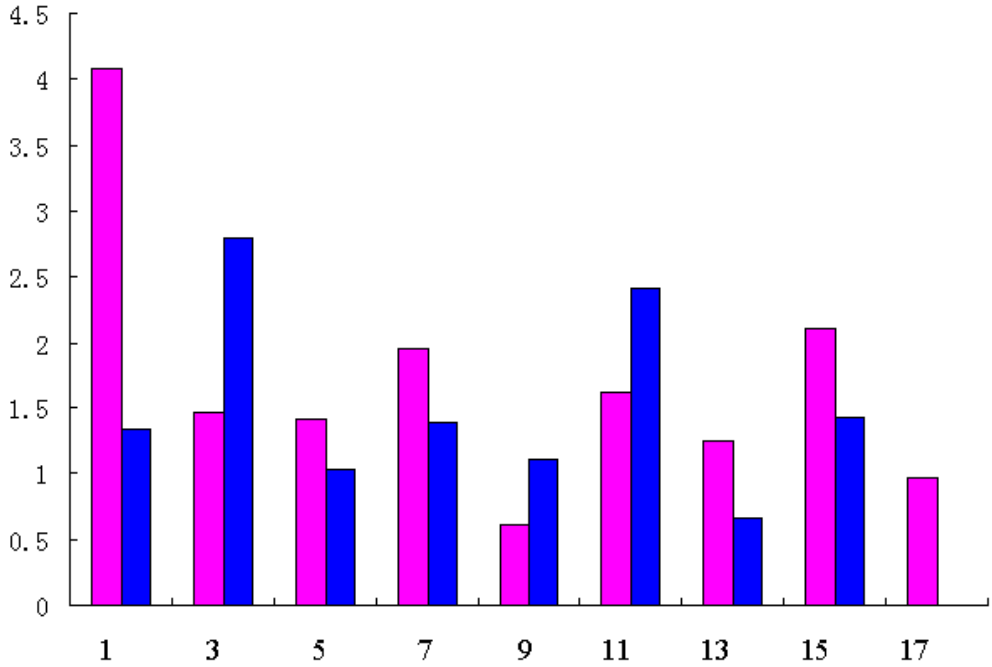

Fig. 5.3.6-1 Sedimentation rate during the past glacial/interglacial stages, MIS stage is shown by numbers below.

The random results do not consistent with the published results that sedimentation rates in the Arctic Ocean increased during glaciations (Worm, 1997). The possibility of relative deposition speed in two closing glacial/interglacial stages is almost equally appeared during the past 735 ka. The result again prove that none glacial or interglacial stages are repeatable.

6. Discussion

6.1. Climate factors and RPI

SINT-800 and RPI has both been correlated with $\delta^{18}O‰$ (ODP677, from Løvlie) curve. The pretty good fit of SINT-800 and $\delta^{18}O$ show that the paleointensity is affected by climate variation. Intervals of higher paleointensity correspond with lower temperatures, while lower intensities corresponds with higher temperatures (see purple and pink lines in Fig. 6.1).

However, the RPI we have derived does not always fit the $\delta^{18}O‰$ curve in this simple way.

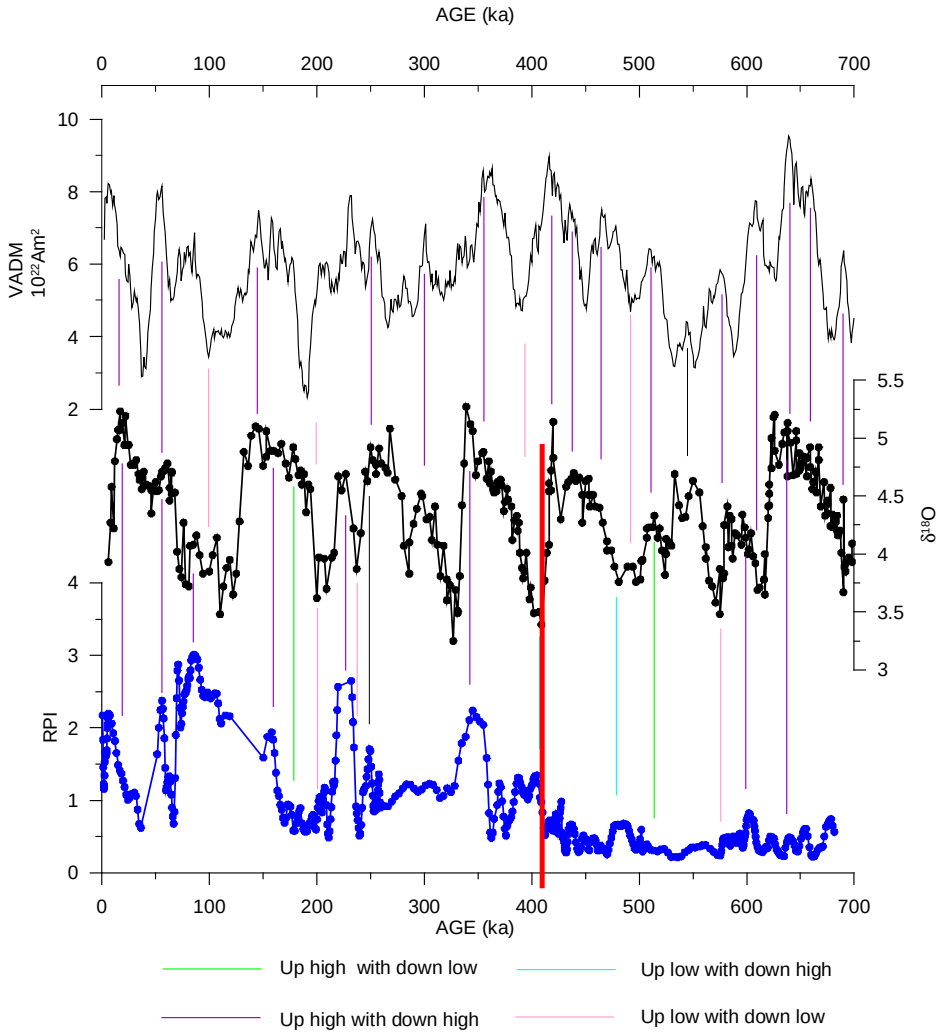

Fig.6.1 SINT-800 & RPI correlated with MIS (ODP 677). Lines with four different colors represent four possibilities of correspondence.

Along most of the core RPI and $^{18}O/^{16}O$ vary in accord, especially before around 410ka (620 cm, from where the RPI low commences, the red line in Fig.6.1). At a few levels, RPI and $^{18}O/^{16}O$ show inverse relationship. The age-depth model may not be so reliable due to the low RPI magnitude below around 620 cm.

A correspond between RPI and $^{18}O/^{16}O$ has been noted by Worm (1997).

Consider the mainly dipolar structure of the geomagnetic field, the strength of the field should vary similarly at the same location. Therefore, the applied normalization of the NRM intensity by rock magnetic parameters (susceptibility, ARM or IRM) may have been insufficient in removing climatically driven modulations of the rock magnetic properties.

In my study, I propose that rock magnetic properties may have been affect by chemical processes (precipitation of secondary minerals, etc.).

6.2 Regional correlation of seven Alpha Ridge cores

Shipboard whole core magnetic susceptibility (WCMS) enable a detailed stratigraphic correlation with 7 cores collected during HLY-0503 expedition from the Alpha Ridge.

A number of distinct cure patterns may be recognized on all records.

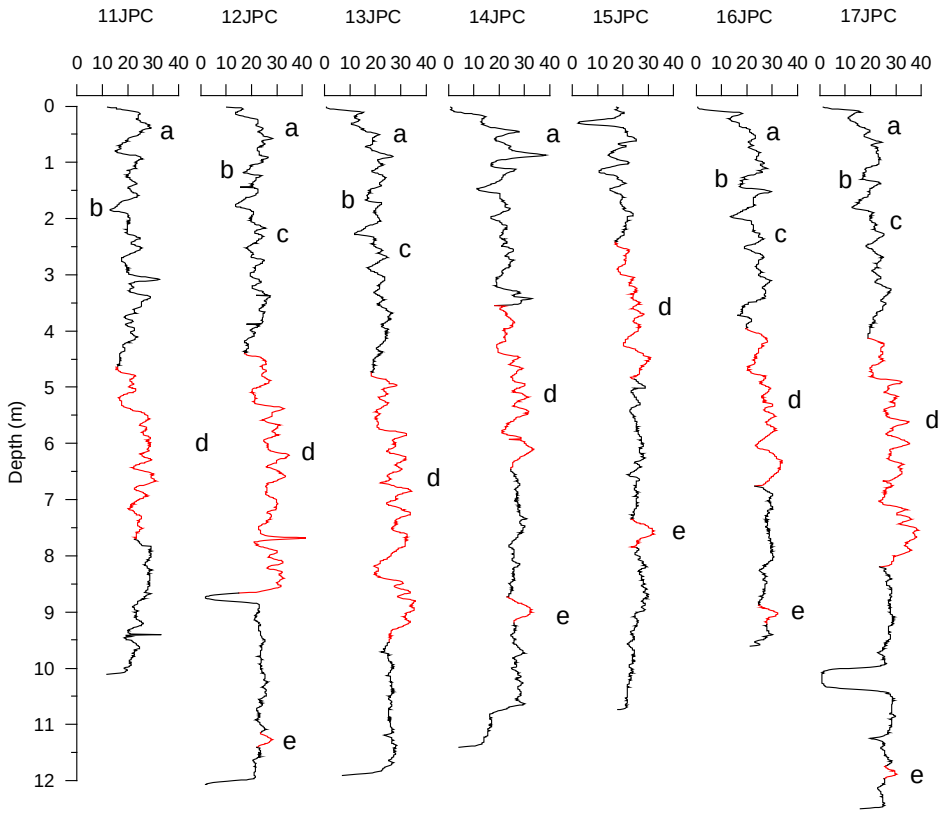

Fig.6.2.1 WCMS feature data points correlation performed among seven JPC cores.

Comparable features are labled a, b, c, d, e (see Fig.6.2.1). Even the thickness are different, feature (d) is conspicuously visible in all 7 cores (see the red lines, lasts around 200 ka), covering a time interval between 236ka and 417 ka (MIS7-MIS11), which suggests a uniform depositional environment during the two glacial cycles (Berger & Loutre, 2007).

According to the proposed age-depth model of JPC-14, the conspicuous feature (d) covers an age of 236 – 417ka see the red tie-lines in figure 6.2.2.

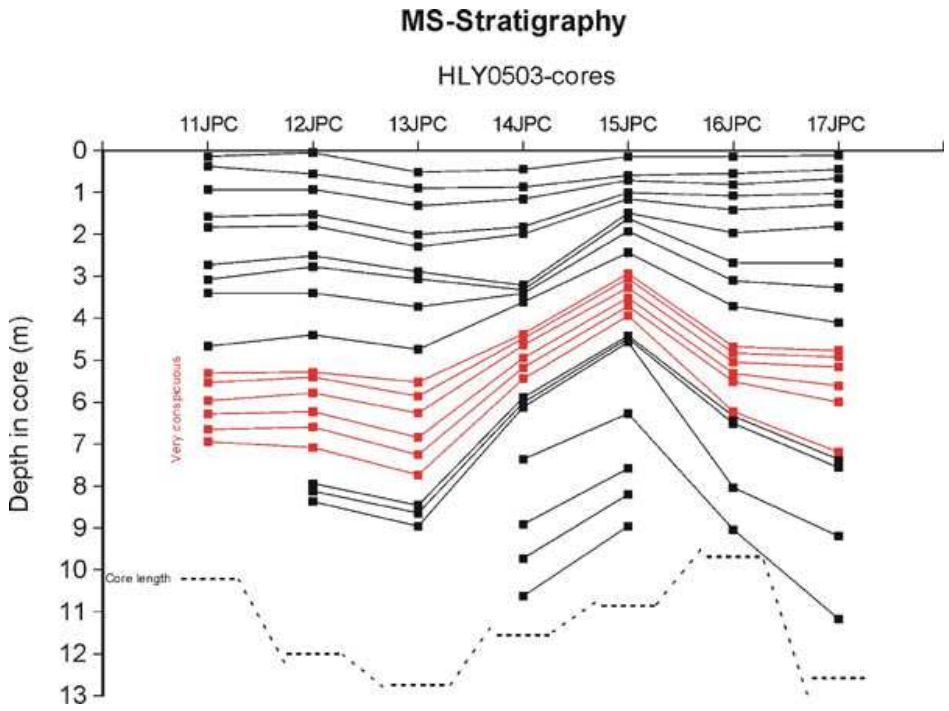

Fig. 6.2.2 Stratigraphy correlation of MS- features of seven cores from the Alpha Ridge (data from Løvlie 2005)

Stratigraphic tie-lines suggest that the cores may be correlated in detail. If one of the seven cores is dated properly, the age of Alpha Ridge sediments can be indicated as well.

7. Conclusions

1) The intervals of inferred negative inclination are too long to be accounted by geomagnetic excursions.
2) Intervals of negative inclinations are not always associated with RPI-lows.
3) On the assumption that RPI in JPC-14 is a genuine reflection of geomagnetic field intensity variation, a correlation with SINT-800 is performed.
4) Correlation between RPI of JPC-14 and SINT-800 combined with FAD of E. Huxleyi results in an age-depth model suggesting the mean sedimentation rate of 1.48 cm/ka.
5) The age-depth model implies an age of JPC-14 of 735ka.
6) The negative inclinations may not suggest geomagnetic field excursions, most probably they represent unresolved remagnetization by chemical processes.
7) Rock magnetic properties with inferred glacial/interglacial intervals apparently suggest some dependence of climate.
8) Correlating RPI with the $\delta^{18}O‰$ curve, it appears that the RPI may be partly affected by climate factors.
9) Combined with the WCMS data of seven cores from the Alpha-Ridge, the age-depth model can be used to estimate the age of other cores based on the regional stratigraphy deduced from the widely developed conspicuous features.

Acknowledgements

I would like to express my gratitude to all those who gave me the possibility to complete this thesis. I want to thank my supervisor professor Reidar Løvlie for helping me on the way of the master's program. His scientific mind, valuable suggestions and effective guidance really benefit me a lot not only in study, but also in life. I want to thank Harald Walderhaug for his lectures, patient help and useful suggestions as well.

Thanks also to the department of earth science, University of Bergen for providing good conditions for studying, reliable instruments and good library service.

A great thanks to Elin Jarland Eriksen, Norbjørg Kaland, Kristin Miskov Nodland and everybody at the Department for their help and assistance in daily issues.

I am also grateful to Statens Lånekassen for the financial support I have received as a Qoata Program student.

Deeply I thank professor Pu Su from Taiyuan University of Technology for invaluable guidance both in my work and also in my life. It was his suggestion that led me to continue my education at the University of Bergen. Thank professor Xingzhao Fan for his help in study.

The experience to stay and study in Bergen I feel has benefited me to be more independent.

Also thanks to my fellow students Junjie Huo, Ronghua Wang and Bin Li for sharing the study room, thoughts, pressures and comfort.

Finally, I would like to give my special thanks to my parents, my sister and brother, who have given me invaluable support by their love that has given me strength and courage through the years.

References

Brook, E.J., Ice core method - Stable isotopes, Encyclopedia of Quaternary Science, 2007, Pages 1212-1219.

Berger, A. & Loutre, M.F., Milankovitch Theory and Paleoclimate, Encyclopedia of Quaternary Science, 2007, Pages 1017-1022.

Backman, J., Jakobsson, M. et. al., Is the central Arctic Ocean a sediment starved basin? Quaternary Science Reviews 23 (2004) 1453-1454.

Bischof, J.F. & Darby, D.A., Mid- to Late Pleistocene ice drift in the western Arctic Ocean: evidence for a different circulation in the past, Science, Vol. 277, 4 July 1997.

Butler R. F., 1991, Paleomagnetism.

Banerjee, S.K., King, J.W. et. al., A rapid method for magnetite granulometry with applications to environmental studies, Geophys. Res. Lett., 8, 333, 336, 1981.

David, J.W., Flood, R.D. , et. al., SYNTHESIS OF STRATIGRAPHIC CORRELATIONS OF THE AMAZON FAN, Proceedings of the Ocean Drilling Program, Scientific Results, Vol. 155, 595, 1997

Guyodo, Y.& Valeet, J. P., Global changes in intensity of the Earth's magnetic field during the past 800 kyr, Nature, Vol. 399, 20 May 1999.

Guyodo, Y.& Valeet, J. P., Relative variations in geomagnetic intensity from sedimentary records: the past 200,000 years, Earth and Planetary Science Letters 143 (1996) 23-36.

Jakobsson, M., Løvlie, R. et. al., Pleistocene stratigraphy and paleoenvironmental variation from Lomonosov Ridge sediments, central Arctic Ocean, Global and Planetary Change 31(2001) 1–22.

Jakobsson, M., Løvlie, R. et. al., Manganese and color cycles in Arctic Ocean sediments constrain Pleistocene chronology, Geology, January 2000, v.28; no. 1; p. 23-26.

Knies, J. & Vogt, Ch., Freshwater pulses in the eastern Arctic Ocean during Saalian and Early Weichselian ice-sheet collapse, Quaternary Research 60 (2003) 243–251.

King, J. W., Banerjee, S. K. and Marvin, J., A new rock-magnetic approach to selecting sediments for geomagnetic paleointensity studies: Application to paleointensity for the last 4000 years, AGU, 1983, p. 3B0431.

Krischvink, J. L., The least-squares line and plane and the analysis of paleomagnetic data. Geophys. J. R. astr. Soc. (1980) 62, 699-718.

Løvlie, R. & Walderhaug, H. J., January 2003, GFJ 280, Paleomagnetic methods, Department of Earth Science, University of Bergen, Norway.

Lund, S., Stoner, J.S., et. al., A summary of Brunhes paleomagnetic field variability recorded in Ocean Drilling Program cores, Physics of the Earth and Planetary Interiors 156 (2006) 194-204.

Løvlie, R., 1989a, Paleomagnetic stratigraphy: a correlation method, Quaternary Journal, 1, 129-149.

Løvlie, R., 1989b. Paleomagnetic excursions during the last interglacial/glacial cycle: a sysnthesis, Quat. Int., ¾, 5-11.

Matthiessen, J., Knies, J. et. al., Late Quaternary dinoflagellate cyst stratigraphy at the Eurasian continental margin, Arctic Ocean: indications for Atlantic water inflow in the past 150,000 years, Global and Planetary Change 31(2001) 65–86.

Nowaczyk, N.R. & Knies, J., Magnetiostratigraphic results from the eatern Arctic Ocean: AMS ^{14}C ages and relative paleointensity data of the Mono Lake and Laschamp geomagntic reversal excursions, Geophys. J. Int. (2000) 140, 185-197.

Nowaczyk, N.R., Frederichs, Th. W., et. al., Magnetostratigraphic data from late Quaternary sediments from the Yermak Plateau, Arctic Ocean: evidence for four geomagnetic polarity events within the last 170 Ka of the Brunhes Chron, Geophys. J. Int. (1994) 117, 453-471.

Rosse, S., Kissel, C. et. al., Holocene centennial to millennial-scale climatic variability: evidence from high-resolution magnetic analyses of the last 10 cal kyr off North Iceland (core MD99-2275), Earth and Planetary Science Letters 242 (2006) 390-405.

Sagnotti, Roberts A.P. et. al., Apparent magnetic polarity reversals due to remagnetization resulting from late diagenetic growth of greigite from siderite, Geophys. J.Int. (2005) 160, 89-100.

Smith, L. M., Millera, G. H. et. al., Sensitivity of the Northern Hemisphere climate system to extreme changes in Holocene Arctic sea ice, Quaternary Science Reviews 22 (2003) 645–658.

Thouveny, N., Carcaillet, J. et. al., Geomagnetic moment variation and paleomagnetic excursions since 400 kyr BP: a stacked record from sedimentary sequences of the Portuguese margin, Earth and Planetary Science Letters 219 (2004) 377-396.

Valet, J. P. & Meynadier, L., A comparison of different techniques for relative paleointensity, Geophysical Research Letters, Vol. 25, No. 1, P. 89-92, 1 January, 1998.

Valet, J. P. & Meynadier, L., Geomagnetic feild intensity and reversals during the last four million years. Nature 366, 234-238.

Worm, H. U., A link between geomagnetic reversals and events and glaciations, Earth and Planetary Science Letters 147 (1997) 55-67.